Electronic Supplementary Material (ESI) for Materials Chemistry Frontiers.

Supplementary information

Topology-guided functional multiplicity of iron-based metal-organic frameworks

Erika Virmani,[a] Ole Beyer,[b] Ulrich Lüning,[b] Uwe Ruschewitz[c] and Stefan Wuttke*[a]

---

[a] Department of Chemistry and Center for NanoScience (CeNS), LMU Munich, Butenandtstraße 11, D-81377 Munich, Germany

[b] Christian-Albrechts-Universität zu Kiel, Otto Diels-Institut für Organische Chemie, Otto-Hahn-Platz 4, D-24118 Kiel, Germany

[c] Universität zu Köln, Institut für Anorganische Chemie, Greinstr. 6, D-50939 Köln, Germany

*Correspondence to:
stefan.wuttke@cup.uni-muenchen.de

Table of Contents

Abbreviations

BDC	1,4-benzenedicarboxylic acid
BET	Brunauer-Emmett-Teller
BPDC	biphenyl-4,4'-dicarboxylic acid
BTB	4,4′,4″,-benzene-1,3,5-triyl-tris(benzoic acid)
DSC	differential scanning calorimetry
EA	elemental analysis
EDX	energy dispersive X-ray
M	molar
PXRD	powder X-ray diffractrogram
SEM	scanning electron microscopy
TAPB	2,4-bis(4’-carboxy-biphenyl-4-yl)-6-(4’-carboxy-2-methoxy-biphenyl-4-yl]-1,3,5-triazine
TATB	4,4',4''-(1,3,5-triazine-2,4,6-triyl)tribenzoic acid
TGA	thermogravimetric analysis

1. Characterization Techniques

Powder X-ray diffraction (PXRD): On a STOE Stadi MP diffractometer, the X-ray diffraction data were recorded using the transmission geometry mode. The X-ray was Ge-filtered Cu $K_{\alpha1}$ (λ = 1.54060 Å) and generated at 40 kV and 40 mA. A DECTRIS MYTHEN 1K strip solid-state detector was used to detect the reflections. The sample was placed in the sample holder between two 0.014 mm thick acetate-foils (ultraphan) in the sample holder. In an omega-2-theta scanning mode, the diffraction patterns were collected using a step size of 4.71° and a counting time of 60 s per step between 2.00 – 44.375°. For the refinement, the diffraction pattern was also collected in an omega-2-theta scanning mode with a step size of 4.71° and a counting time of 60 s per step between 2.000 – 91.400°, 2.005 – 91.405° and 2.010 – 91.410°. Afterwards the patterns were merged together.

Synchrotron PXRD: High-resolution synchrotron powder diffraction data were recorded at the Swiss Norwegian BeamLine (SNBL BM01B) at the European Synchrotron at Grenoble/France (ESRF).[1] The wavelength was calibrated with a Si standard NIST 640c to 0.504477 Å. The diffractometer is equipped with five counting channels, delivering five complete patterns collected simultaneously with a small 1.1° offset in 2θ. A Si(111) analyzer crystal was mounted in front of each NaI scintillator/photomultiplier detector. Data were collected at room temperature (Fe-TATB-BDC-a, -b, -c, -e) and 100 K (Fe-TATB-BDC-a, -e) between 0° and 20°/25° in 2θ with steps of 0.002° and 100 ms integration time per data point (approx. 20 min for one scan). This scanning procedure was repeated several times and the resulting data from all detectors and measurements were averaged into one pattern (Table S8, and Figure S32) with local software. Samples were after activation sealed in glass capillaries (∅ 1.0 mm) in an argon atmosphere.

Analysis of PXRD data: *Rietveld* refinements of the resulting PXRD data with the published structural data of MIL-142 and MIL-143[2] as starting parameters turned out to be unstable. This is not surprising for the laboratory PXRD data, as the non-activated samples contain electron density within their pores, which is always difficult to be modelled. But also for the synchrotron data recorded on activated samples no stable refinements were obtained obviously due to the large unit cells and relatively low statistics of the measurements, which seems to be reasonably lower than that given by Chevreau *et al.*[2] for MIL-143. Therefore only *Le Bail* fits were performed in space group *F*23 (MIL-143 topology) or *R*3*c* (MIL-142 topology) using the GSAS software.[3] The published lattice parameters of MIL-142 and MIL-143 were used as starting values, the resulting lattice parameters are summarized in Table S8. The respective *Le Bail* fits are depicted in Figures S32 and S33. After these refinements it was possible to look for possible impurity phases by visual inspection of the resulting fits. This is mainly the MOF of the other topology. This information has also been added to Table S8.

The pattern of as-synthesized Fe-TAPB-BDC (Figure S21) was indexed using the TREOR algorithm allowing only cubic unit cells.[4] The resulting lattice parameter *a* was used as starting value for a *Le Bail* fit in *F*23. The good agreement between the recorded and the calculated pattern confirms the MIL-143 topology also for this compound.

Nitrogen sorption: Prior to the measurement, the materials were degassed at 120 °C in high vacuum for at least 12 h. Nitrogen sorption isotherms were recorded at 77 K with a Quantachrome AUTOSORB-IQ or AUTOSORB-1 instrument. Evaluation of sorption data was carried out using ASiQwin^{TM} software suite (Version 3.0, Quantachrome Instruments). Brunauer-Emmett-Teller (BET) surface areas were calculated in the p/p_0 range from 0.005 to 0.01, according to Quantachrome recommendations,[5, 6] as in this region the linearized form of the BET equation is valid. The total pore volumes were calculated at p/p_0 0.19 and the pore size distributions were calculated from the adsorption isotherms by employing a quenched solid state functional theory (QSDFT, N_2 at 77 K on carbon, slit/cylindrical pore in the adsorption branch).

Scanning electron microscopy (SEM): First the samples were mounted onto an aluminum cylinder with a carbon sticky tape. Secondly the samples were coated with a thin carbon layer by carbon fiber flash evaporation under high vacuum. SEM images were recorded on a FEI Helios G33 UC. The acceleration voltage of 2 kV was produced by a field emission gun.

Thermal properties: Thermogravimetric analysis (TGA) and differential scanning calorimetry (DSC) measurements were determined in parallel using a Netzsch Jupiter ST 449 C instrument equipped with a Netsch TASC 414/4 controller. The samples were loaded into an aluminum oxide crucible and heated from 25 °C to 900 °C with a heating rate of 10 °C min^{-1} under a synthetic air flow (20.5% oxygen in nitrogen from Air Liquide supplier).

Nuclear magnetic resonance (NMR) spectroscopy: ^{1}H-NMR data were recorded on a Bruker DRX 500 spectrometer. The chemical shifts are referenced to the residual proton signal of the solvent.

2. Experimental

2.1 General

[1,1′-Bis(diphenylphosphino)ferrocene]dichloro palladium(II) (99.9 %, ABCR); 2-amino-1,4-benzenedicarboxylic acid (99%, Sigma Aldrich); 4-(methoxycarbonyl)phenylboronic acid (97 %, ABCR); biphenyl-4,4'-dicarboxylic acid (97%, Sigma Aldrich); iron(III) chloride hexahydrate ($FeCl_3 \cdot 8\ H_2O$, analysis grade, in-house supply); methanol (anhydrous, 99.8%, Sigma Aldrich); *N*,*N*-dimethylformamide (anhydrous, synthesis grade, Fischer Scientific); 1,4-benzendicarboxylic acid (98%, Sigma Aldrich).

2.2 Linker synthesis

2-(4-Bromo-3-methoxyphenyl)-4,6-bis(4-bromophenyl)-1,3,5-triazine: 2-(4-Bromo-3-methoxyphenyl)-4,6-bis(4-bromophenyl)-1,3,5-triazine was prepared according to the literature procedure.[7]

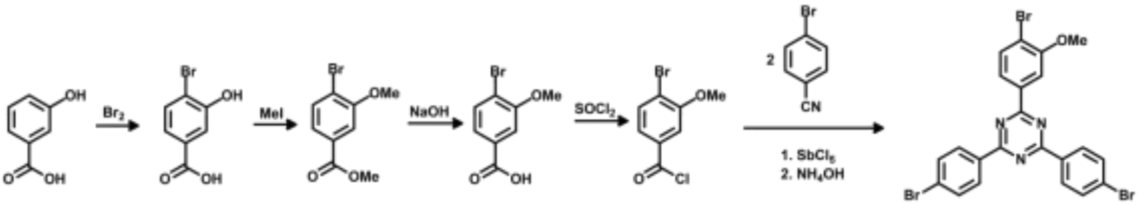

Figure S1: Illustration of the synthetic route to obtain mono-substituted methoxy-functionalized triazine-based trigonal linker for the synthesis of the elongated version of TATB.

2,4-Bis[4’-(methoxycarbonyl)-biphenyl-4-yl]-6-[2-methoxy-4’-(methoxycarbonyl)-biphenyl-4-yl]-1,3,5-triazine (7)

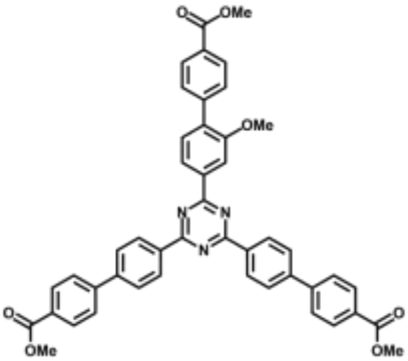

Under nitrogen atmosphere, 2-(4-bromo-3-methoxyphenyl)-4,6-bis(4-bromophenyl)-1,3,5-triazine (**5**, 5.00 g, 8.68 mmol), 4-methoxycarbonyl-phenylboronic acid (**6**, 6.10 g, 33.9 mmol), [1,1′-bis(diphenylphosphino) ferrocene] dichloro palladium(II) (635 mg, 868 µmol) and potassium phosphate (16.6 g, 78.1 mmol) were suspended in 1,4-dioxane (300 mL) and deionized water (30 mL). The mixture was stirred for 72 h at 120 °C and the solvent was evaporated in vacuo. Ethyl acetate (400 mL) and deionized water (100 mL) were added to the residue. The organic layer was separated, washed with water (3 x 100 mL) and brine (1 x 100 mL) and dried with magnesium sulphate. The solvent was evaporated in vacuo and the residue was recrystallized from a mixture of toluene and *n*-heptane. A colourless solid was obtained. Yield: 4.1 g (4.94 mmol, 57 %).

^{1}H-NMR (500 MHz, 300 K, CDCl$_{3,}$): δ = 8.88 (d, 4H, ^{3}J = 8.4 Hz, 2,4-Ar-*H*-2,6), 8.50 (dd, 1H, ^{3}J = 7.9 Hz, ^{4}J = 1.4 Hz, 6-Ar-*H*-5), 8.43 (d, 1H, ^{4}J = 1.4 Hz, 6-Ar-*H*-3), 8.17 (d, 4H, ^{3}J = 8.4 Hz, 2,4-Ar’-*H*-3,5), 8.13 (d, 2H, ^{3}J = 8.4 Hz, 6-Ar’-*H*-3,5), 7.86 (d, 4H, ^{3}J = 8.4 Hz, 2,4-Ar-*H*-3,5), 7.78 (d, 4H, ^{3}J = 8.4 Hz, 2,4-Ar’-*H*-2,6), 7.71 (d, 2H, ^{3}J = 8.4 Hz, 6-Ar’-*H*-2,6), 7.56 (d, 1H, ^{3}J = 7.9 Hz, 6-Ar-*H*-6), 4.04 (s, 3H, OC*H*$_{3}$), 3.97 (s, 6H, 2,4-Ar’-CO$_{2}$C*H*$_{3}$), 3.96 (s, 3H, 6-Ar’-CO$_{2}$C*H*$_{3}$) ppm.

2,4-Bis(4’-carboxy-biphenyl-4-yl)-6-(4’-carboxy-2-methoxy-biphenyl-4-yl)-1,3,5-triazine (8)

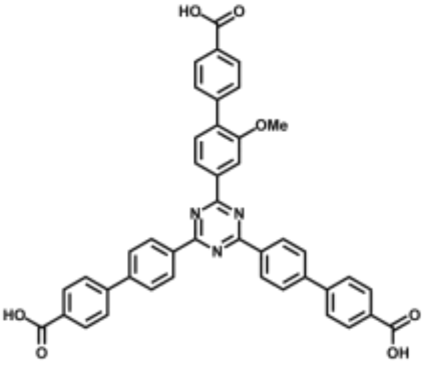

2,4-Bis[4’-(methoxycarbonyl)-biphenyl-4-yl)-6-[2-methoxy-4’-(methoxycarbonyl)-biphenyl-4-yl]-1,3,5-triazine (**7**, 3.00 g, 4.04 mmol) was mixed with 2 M aqueous sodium hydroxide (200 mL) and 1,4-dioxane (10 mL). The suspension was stirred for 12 h at 120 °C and became a clear solution. The reaction mixture was acidified with concentrated hydrochloric acid (200 mL) and the resulting precipitate was filtered off and washed with deionized water. A colorless solid was obtained. Yield: 2.74 g (3.92 mmol, 97 %).

^{1}H-NMR (500 MHz, 300K, DMSO-*d*$_{6}$): δ = 13.02 (br. s, 3H, CO$_{2}$*H*), 8.71 (d, 4H, ^{3}J = 8.4 Hz, 2,4-Ar-*H*-3,5), 8.33 (dd, 1H, *J* = 7.9 Hz, ^{4}J = 1.1 Hz, 6-Ar-*H*-5), 8.27 (d, 1H, ^{4}J = 1.1 Hz, 6-Ar-*H*-3), 8.04 (d, 4H, ^{3}J = 8.4 Hz, 2,4-Ar’-*H*-3,5), 8.00 (d, 2H, ^{3}J = 8.3 Hz, 6-Ar’-*H*-3,5), 7.91 (d, 4H, ^{3}J = 8.4 Hz, 2,4-Ar-*H*-2,6), 7.85 (d, 4H, ^{3}J = 8.4 Hz, 2,4-Ar’-*H*-2,6), 7.65 (d, 2H, ^{3}J = 8.3 Hz, 6-Ar’-*H*-2,6), 7.56 (d, 1H, ^{3}J = 7.9 Hz, 6-Ar-*H*-6), 3.95 (s, 3H, OC*H*$_{3}$) ppm.

2.3 Synthesis of iron(III) based MOFs exhibiting different linker topologies

Fe-TATB-BDC-a: A glass bottle (Schott Duran culture tube, Borosilicate, 5 mL) with a PBT cap equipped with a Teflon seal was used. $FeCl_3 \cdot 6\ H_2O$ (60.0 mg, 0.222 mmol) was dissolved in DMF (1 mL) via ultrasonication. TATB acid (**4a**, 48.6 mg, 0.110 mmol) and 1,4-benzendicarboxylic acid (36.6 mg, 0.220 mmol) were added and dissolved via ultrasonication. The reaction mixture was placed in an oven and heated to 150 °C within 1 h, kept at this temperature for 20 h and afterwards slowly cooled down to room temperature within 1 h. The solid was isolated by centrifugation (Eppendorf centrifuge 5430, 7830 rpm, 5 min) and washed via suspension in DMF (10 mL) and subsequent centrifugation. Suspension and centrifugation were repeated three times. The isolated brick-red powdery solid was dried in vacuum ($2.4 \cdot 10^{-3}$ bar) for 6 h. The sample was extracted with methanol (4 Å molecular sieve was added to methanol phase) under nitrogen atmosphere using a Soxhlet device (5 mL) for 72 h. The powder (41.5 mg, 40%) was dried in vacuum ($2.4 \cdot 10^{-3}$ bar) for 6 h and afterwards the sample was stored under nitrogen atmosphere at room temperature.

Fe-TATB-BDC-b: A glass bottle (Schott Duran culture tube, Borosilicate, 5 mL) with a PBT cap equipped with a Teflon seal was used. $FeCl_3 \cdot 6\ H_2O$ (60.0 mg, 0.222 mmol) was dissolved in DMF (1 mL) via ultrasonication. TATB acid (**4a**, 48.6 mg, 0.110 mmol) and 2-amino-1,4-benzenedicarboxylic acid (40.2 mg, 0.220 mmol) were added and dissolved via ultrasonication. The reaction mixture was placed in an oven and heated to 150 °C within 1 h, kept at this temperature for 20 h and afterwards slowly cooled down to room temperature within 1 h. The solid was isolated by centrifugation (Eppendorf centrifuge 5430, 7830 rpm, 5 min) and washed via suspension in DMF (10 mL) and subsequent centrifugation. Suspension and centrifugation were repeated three times. The isolated light brown powdery solid was dried under vacuum ($2.4 \cdot 10^{-3}$ bar) for 6 h. The sample was extracted with methanol (4 Å molecular sieve was added to methanol phase) under nitrogen atmosphere using a Soxhlet device (5 mL) for 72 h. The powder (46.5 mg, 44%) was dried in vacuum ($2.4 \cdot 10^{-3}$ bar) for 6 h and afterwards the sample was stored under nitrogen atmosphere at room temperature.

Fe-TATB-BDC-c: A glass bottle (Schott Duran culture tube, Borosilicate, 5 mL) with a PBT cap equipped with a Teflon seal was used. $FeCl_3 \cdot 6\ H_2O$ (60.0 mg, 0.222 mmol) was dissolved in DMF (1 mL) via ultrasonication. TATB-NO_2(meta) acid (**4b**, 53.5 mg, 0.110 mmol) and 1,4-benzenedicarboxylic acid (36.6 mg, 0.220 mmol) were added and dissolved via ultrasonication. The reaction mixture was placed in an oven and heated to 150 °C within 1 h, kept at this temperature for 20 h and afterwards slowly cooled down to room temperature within 1 h. The solid was isolated by centrifugation (Eppendorf centrifuge 5430, 7830 rpm, 5 min) and washed via suspension in DMF (10 mL) and subsequent centrifugation. Suspension and centrifugation were repeated three times. The isolated orange powdery solid was dried under vacuum ($2.4 \cdot 10^{-3}$ bar) for 6 h. The sample was extracted with methanol (4 Å molecular sieve was added to methanol phase) under nitrogen atmosphere using a Soxhlet device (5 mL) for 72 h. The powder (38.2 mg, 35%) was dried in vacuum ($2.4 \cdot 10^{-3}$ bar) for 6 h and afterwards the sample was stored under nitrogen atmosphere at room temperature.

Fe-TATB-BDC-d: A glass bottle (Schott Duran culture tube, Borosilicate, 5 mL) with a PBT cap equipped with a Teflon seal was used. $FeCl_3 \cdot 6\ H_2O$ (60.0 mg, 0.222 mmol) was dissolved in DMF (1 mL) via ultrasonication. TATB-NO_2(ortho) acid (**4c**, 53.5 mg, 0.110 mmol) and 1,4-benzenedicarboxylic acid (36.6 mg, 0.220 mmol) were added and dissolved via ultrasonication. The reaction mixture was placed in an oven and heated to 150 °C within 1 h, kept at this temperature for 20 h and afterwards slowly cooled down to room temperature within 1 h. The solid was isolated by centrifugation (Eppendorf centrifuge 5430, 7830 rpm, 5 min) and washed via suspension in DMF (10 mL) and subsequent centrifugation. Suspension and centrifugation were repeated three times. The isolated dark brown powdery solid was dried under vacuum ($2.4 \cdot 10^{-3}$ bar) for 6 h. The sample was extracted with methanol (4 Å molecular sieve was added to methanol phase) under nitrogen atmosphere using a Soxhlet device (5 mL) for 72 h. The powder (39.6 mg, 36%) was dried in vacuum ($2.4 \cdot 10^{-3}$ bar) for 6 h and afterwards the sample was stored under nitrogen atmosphere at room temperature.

Fe-TATB-BDC-e: A glass bottle (Schott Duran culture tube, Borosilicate, 5 mL) with a PBT cap equipped with a Teflon seal was used. $FeCl_3 \cdot 6\ H_2O$ (60.0 mg, 0.222 mmol) was dissolved in DMF (1 mL) via ultrasonication. TATB-NO_2(meta) acid (**4b**, 53.5 mg, 0.110 mmol) and 2-amino-1,4-benzenedicarboxylic acid (40.2 mg, 0.222 mmol) were added and dissolved via ultrasonication. The reaction mixture was placed in an oven and heated to 150 °C within 1 h, kept at this temperature for 20 h and afterwards slowly cooled down to room temperature within 1 h. The solid was isolated by centrifugation (Eppendorf centrifuge 5430, 7830 rpm, 5 min) and washed via suspension in DMF (10 mL) and subsequent centrifugation. Suspension and centrifugation were repeated three times. The isolated light brown powdery solid was dried under vacuum ($2.4 \cdot 10^{-3}$ bar) for 6 h. The sample was extracted with methanol (4 Å molecular sieve was added to methanol phase) under nitrogen atmosphere using a Soxhlet device (5 mL) for 72 h. The powder (63.1 mg, 57%) was dried in vacuum ($2.4 \cdot 10^{-3}$ bar) for 6 h and afterwards the sample was stored under nitrogen atmosphere at room temperature.

Fe-TATB-BPDC: A glass bottle (Schott Duran culture tube, Borosilicate, 5 mL) with a PBT cap equipped with a Teflon seal was used. $FeCl_3 \cdot 6\, H_2O$ (60.0 mg, 0.222 mmol) was dissolved in DMF (1 mL) by ultrasonic treatment. TATB acid (**4a**, 48.6 mg, 0.110 mmol) and biphenyl-4,4'-dicarboxylic acid (53.3 mg, 0.220 mmol) were added and dissolved through ultrasonic treatment. The reaction mixture was placed in an oven and heated to 150 °C within 1 h, kept at this temperature for 20 h and afterwards slowly cooled down to room temperature within 1 h. The solid was isolated bycentrifugation (Eppendorf centrifuge 5430, 7830 rpm, 5 min) and washed via suspension in DMF (10 mL) and subsequent centrifugation. Suspension and centrifugation were repeated three times. The isolated red brown powdery solid (24.9 mg, 21%) was dried in vacuum ($2.4 \cdot 10^{-3}$ bar) for 6 h and stored under nitrogen atmosphere at room temperature.

Fe-TAPB-BDC: A glass bottle (Schott Duran culture tube, Borosilicate, 5 mL) with a PBT cap equipped with a Teflon seal was used. $FeCl_3 \cdot 6\, H_2O$ (60.0 mg, 0.222 mmol) was dissolved in DMF (1 mL) via ultrasonication. TAPB acid (**8**, 77.7 mg, 0.110 mmol) and 1,4-benzenedicarboxylic acid (36.6 mg, 0.220 mmol) were added and dissolved via ultrasonication. The reaction mixture was placed in an oven and heated to 150 °C within 1 h, kept at this temperature for 20 h and afterwards slowly cooled down to room temperature within 1 h. The solid was isolated by centrifugation (Eppendorf centrifuge 5430, 7830 rpm, 5 min) and washed via suspension in DMF (10 mL) and subsequent centrifugation. Suspension and centrifugation were repeated three times. The isolated ochre powdery solid (59.6 mg, 45%) was dried in vacuum ($2.4 \cdot 10^{-3}$ bar) for 6 h and stored under nitrogen atmosphere at room temperature.

Fe-TAPB-BPDC: A glass bottle (Schott Duran culture tube, Borosilicate, 5 mL) with a PBT cap equipped with a Teflon seal was used. $FeCl_3 \cdot 6\, H_2O$ (60.0 mg, 0.222 mmol) was dissolved in DMF (1 mL) via ultrasonication. TAPB acid (**8**, 77.7 mg, 0.110 mmol) and biphenyl-4,4'-dicarboxylic acid (53.3 mg, 0.220 mmol) were added and dissolved via ultrasonication. The reaction mixture was placed in an oven and heated to 150 °C within 1 h, kept at this temperature for 20 h and afterwards slowly cooled down to room temperature within 1 h. The solid was isolated by centrifugation (Eppendorf centrifuge 5430, 7830 rpm, 5 min) and washed via suspension in DMF (10 mL) and subsequent centrifugation. Suspension and centrifugation were repeated three times. The isolated yellow powdery solid (26.9 mg, 19%) was dried in vacuum ($2.4 \cdot 10^{-3}$ bar) for 6 h and stored under nitrogen atmosphere at room temperature.

Fe-BTB-BDC: A glass bottle (Schott Duran culture tube, Borosilicate, 5 mL) with a PBT cap equipped with a Teflon seal was used. $FeCl_3 \cdot 6\,H_2O$ (405 mg, 1.50 mmol) was dissolved in DMF (3 mL) via ultrasonication. 4,4′,4″,-benzene-1,3,5-triyl-tris(benzoic acid) (292 mg, 0.660 mmol) and 1,4-benzenedicarboxylic acid (83.0 mg, 0.500 mmol) were added and dissolved via ultrasonication. The reaction mixture was placed in an oven and heated to 150 °C within 1 h, kept at this temperature for 20 h and afterwards slowly cooled down to room temperature within 1 h. The solid was isolated by centrifugation (Eppendorf centrifuge 5430, 7830 rpm, 5 min) and washed via suspension in DMF (10 mL) and subsequent centrifugation. Suspension and centrifugation were repeated three times. The isolated orange-yellow powdery solid was dried under vacuum ($2.4 \cdot 10^{-3}$ bar) for 6 h. The sample was extracted with methanol (4 Å molecular sieve was added to methanol phase) under nitrogen atmosphere using a Soxhlet device (5 mL) for 72 h. The powder (280 mg, 56%) was dried in vacuum ($2.4 \cdot 10^{-3}$ bar) for 6 h and afterwards the sample was stored under nitrogen atmosphere at room temperature.

2.4 Stability tests

The sample was tested against water, 1 M hydrochloric acid, and 1 M sodium hydroxide. An Eppendorf tube was filled with 5 mg of the MOF sample and 500 µL of either Millipore water, 1 M hydrochloric acid or 1 M sodium hydroxide were added. The tubes were placed into a Thermo-Shaker (Peglab, TS-100) at 25 °C for a defined period of time, either 1 d, 2 d, 3 d, 7 d or 14 d. Afterwards the samples were centrifuged (Eppendorf centrifuge 5418 R, 14000 rpm, 10 min), the supernatant was pipetted off, and the MOF material was dried in an oven at 100 °C for 3 h before PXRD investigations were carried out.

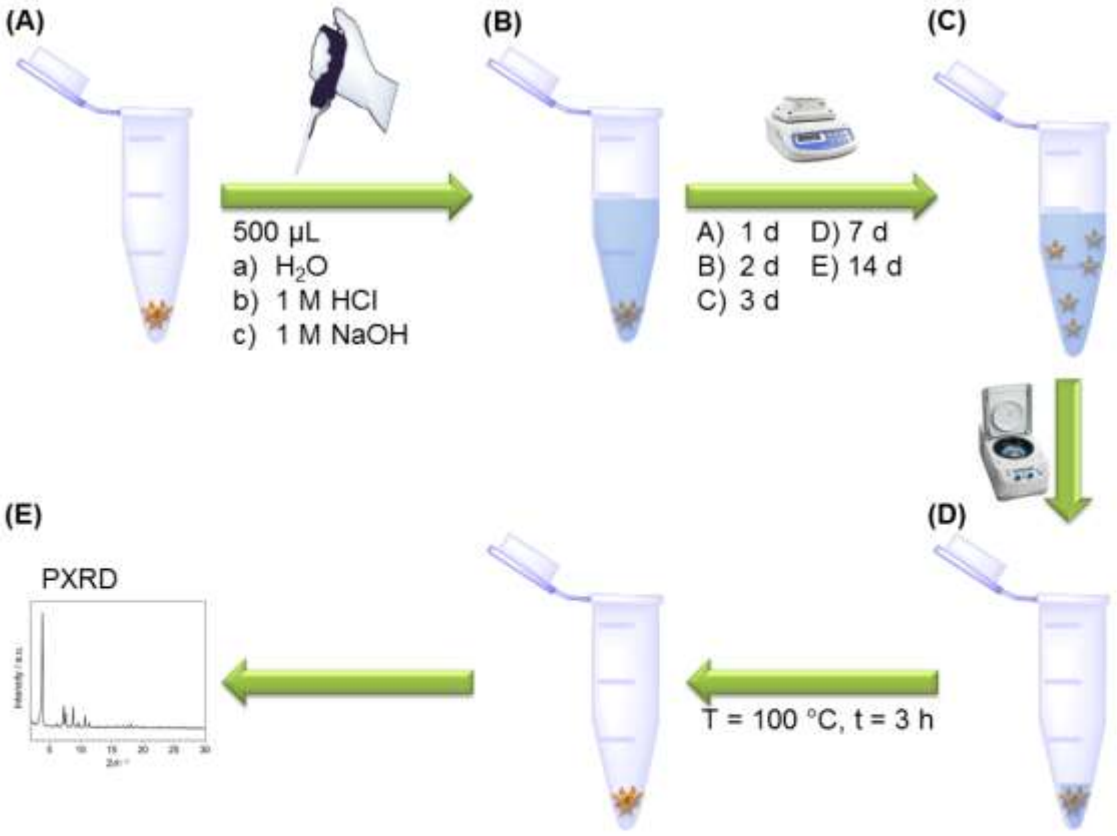

Figure S2: Schematic representation of the strategy for investigating the stability of the MOF samples. The procedure was the following: A) An Eppendorf tube is loaded with 5 mg of the MOF sample and 500 µL either of Millipore water, 1 M hydrochloric acid or 1 M sodium hydroxide were added. B) The mixture was placed on a Thermo-Shaker and shaked at T = 25 °C for either 1 d, 2 d, 3 d, 7 d or 14 d. C) The suspension was centrifuged and the supernatant was pipetted off. D) The resulting wet MOF powder was dried in a preheated oven at T = 100 °C for 3 h. E) The MOF sample was investigated with a PXRD measurement.

3. Figures

2-(4-Bromo-3-methoxyphenyl)-4,6-bis(4-bromophenyl)-1,3,5-triazine (5)

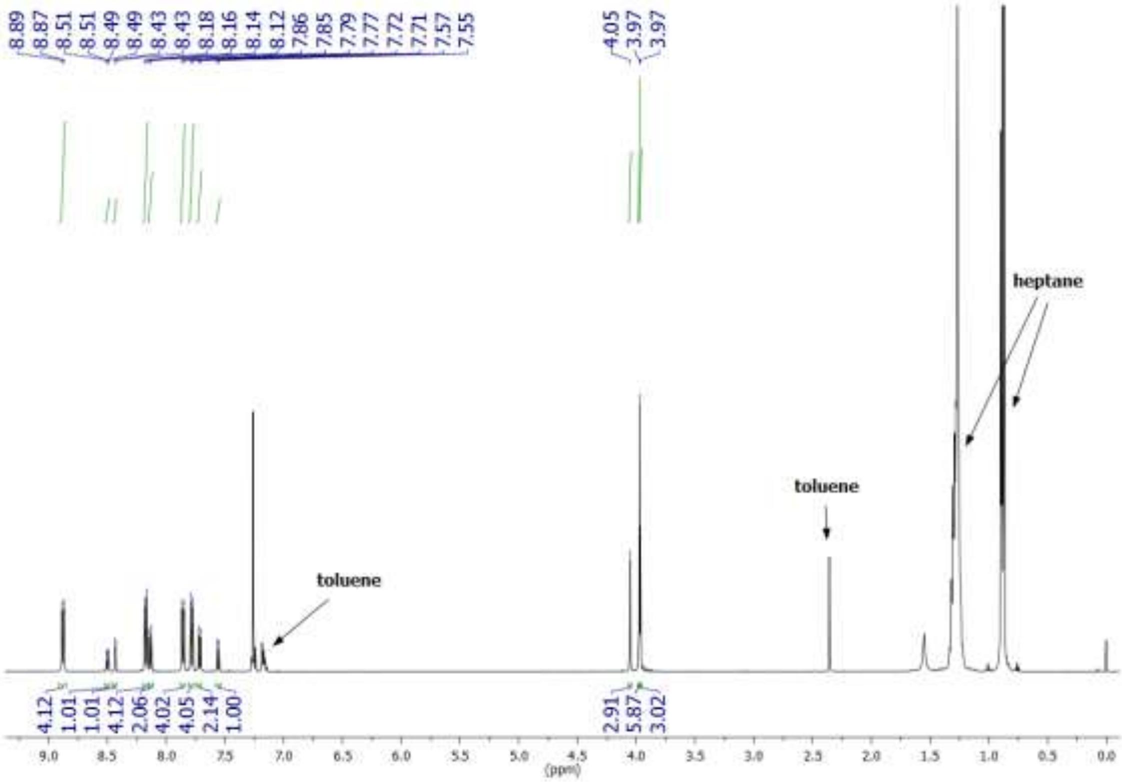

Figure S3: ^{1}H-NMR spectrum (500 MHz, 300 K, $CDCl_3$) of 2-(4-bromo-3-methoxyphenyl)-4,6-bis(4-bromophenyl)-1,3,5-triazine (**5**).

2,4-Bis(4’-carboxy-biphenyl-4-yl)-6-(4’-carboxy-2-methoxy-biphenyl-4-yl)-1,3,5-triazine (8)

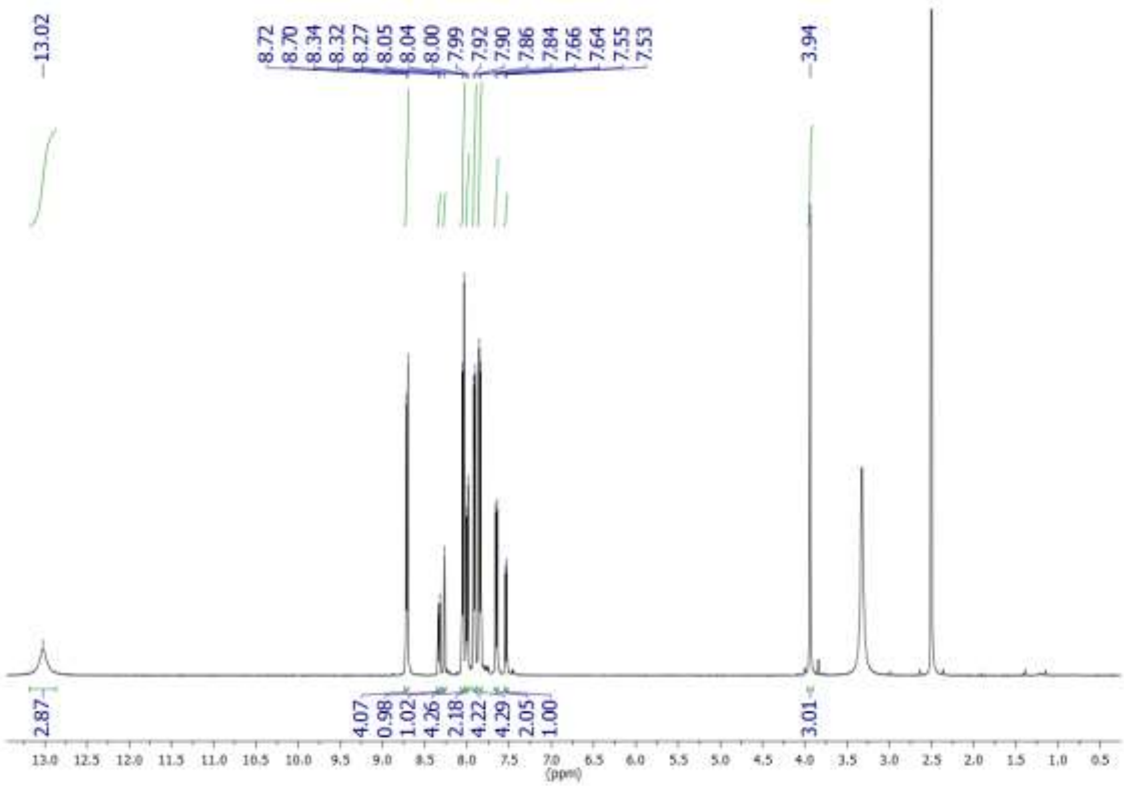

Figure S4: ^{1}H-NMR spectrum (500 MHz, 300 K, DMSO-d$_6$) of 2,4-bis(4’-carboxy-biphenyl-4-yl)-6-(4’-carboxy-2-methoxy-biphenyl-4-yl]-1,3,5-triazine (**8**).

Fe-TATB-BDC-a

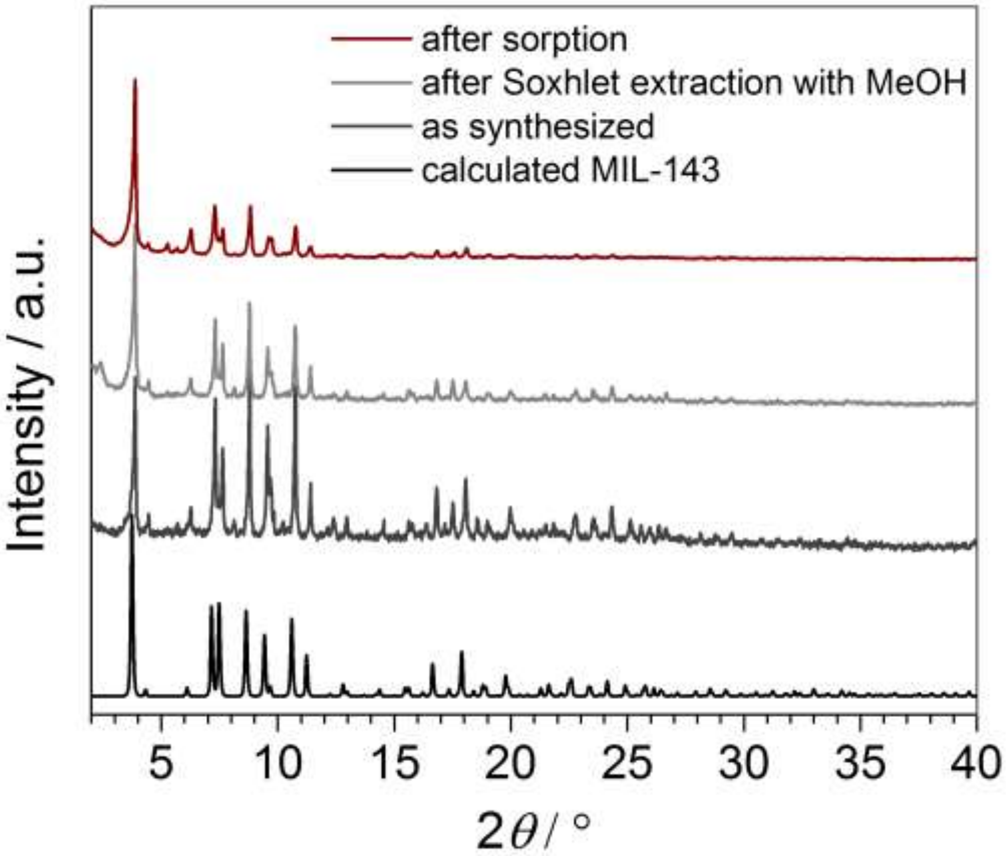

Figure S5: PXRD patterns of Fe-TATB-BDC-a as synthesized (dark gray), after Soxhlet extraction with methanol (light gray), and after sorption isotherm measurement (dark red) are compared to the calculated pattern of MIL-143 (black). All data are from the same synthesis batch.

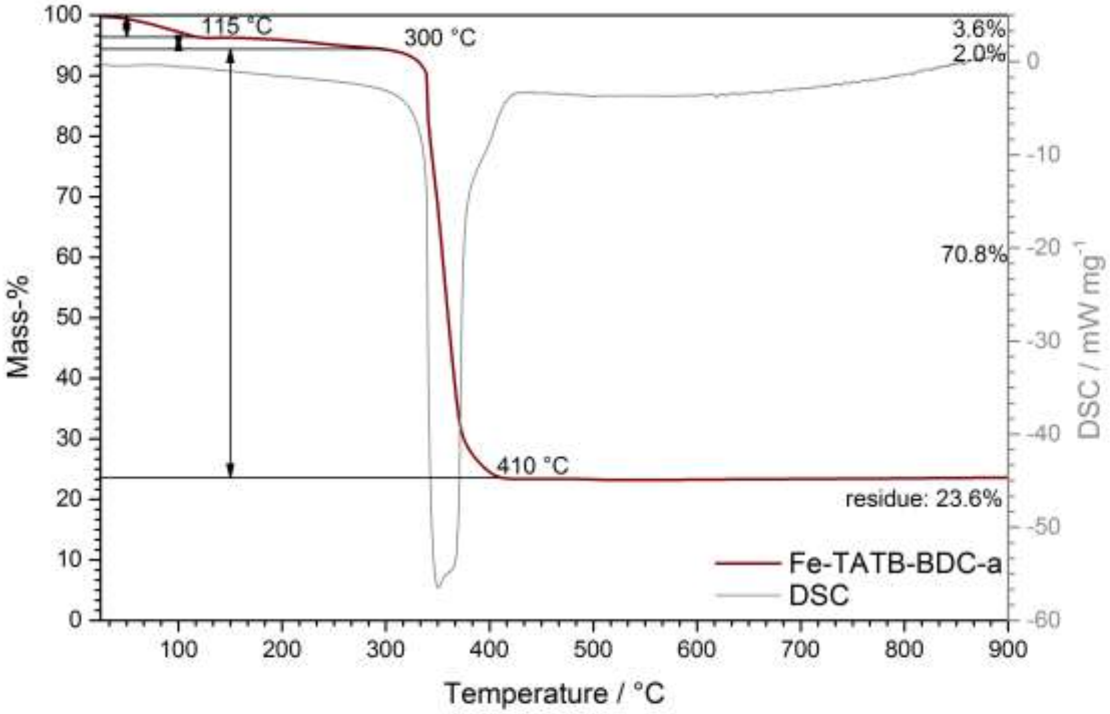

Figure S6: Results of thermogravimetric analysis (dark red curve) and differential scanning calorimetry (light gray curve) of Fe-TATB-BDC-a in flowing air with a heating rate of 10 ^{o}C min^{-1}. Prior to the TGA/DSC measurement, the material had been used for the nitrogen sorption experiments. The start temperature of the decomposition and the mass loss of individual steps are indicated.

Table S1: Mass-losses of Fe-TATB-BDC-a during thermogravimetric analysis: experimentally determined data (Figure S6), experimentally determined data taking the content of guests into account, and calculated data based on the ideal composition of Fe-TATB-BDC-a [$Fe_3O(Cl)(H_2O)_2(BDC)_{3/2}(TATB)$].

	experimental	**guest free**	**calculated**
guest	5.6%		
linker	70.8%	75.0%	74.5%
residue	23.6%	25.0%	25.5%

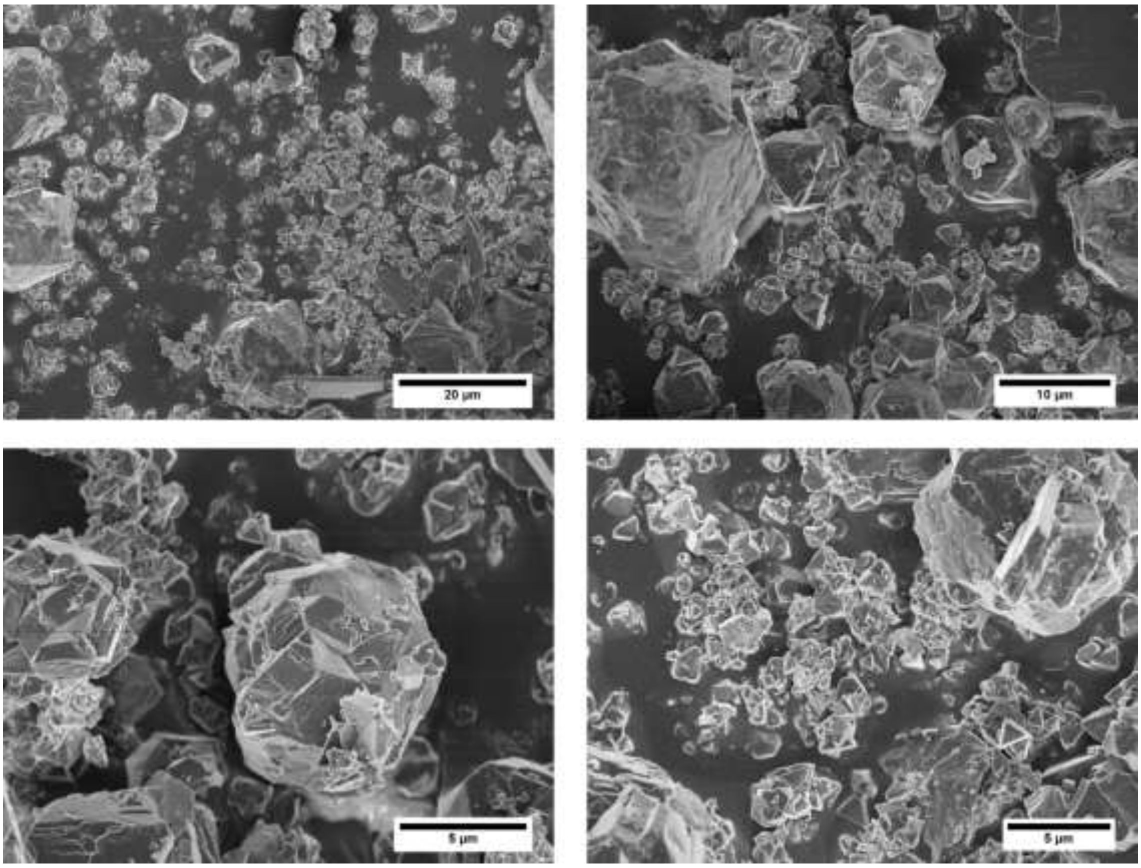

Figure S7: SEM images of the Fe-TATB-BDC-a recorded at different magnifications, showing randomly shaped particles with small and large crystallite sizes.

Fe-TATB-BDC-b

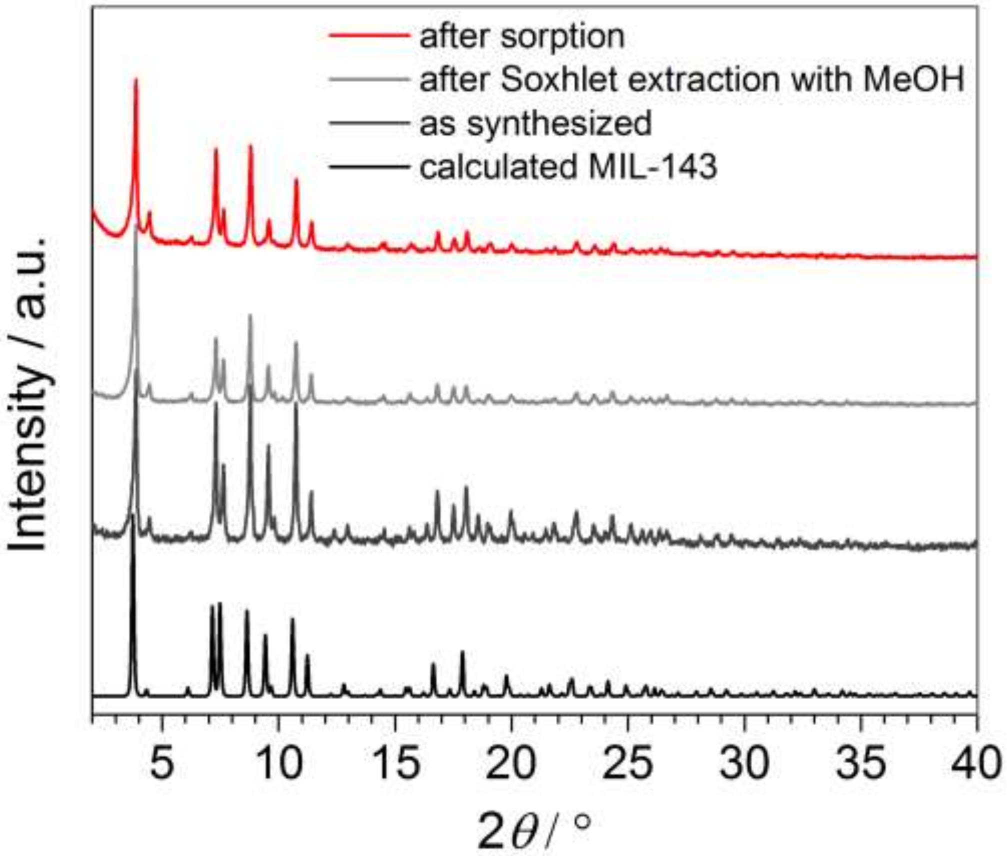

Figure S8: PXRD patterns of Fe-TATB-BDC-b as synthesized (dark gray), after Soxhlet extraction with methanol (light gray), and after sorption isotherm measurement (red) are compared to the calculated pattern of MIL-143 (black). All data are from the same synthesis batch.

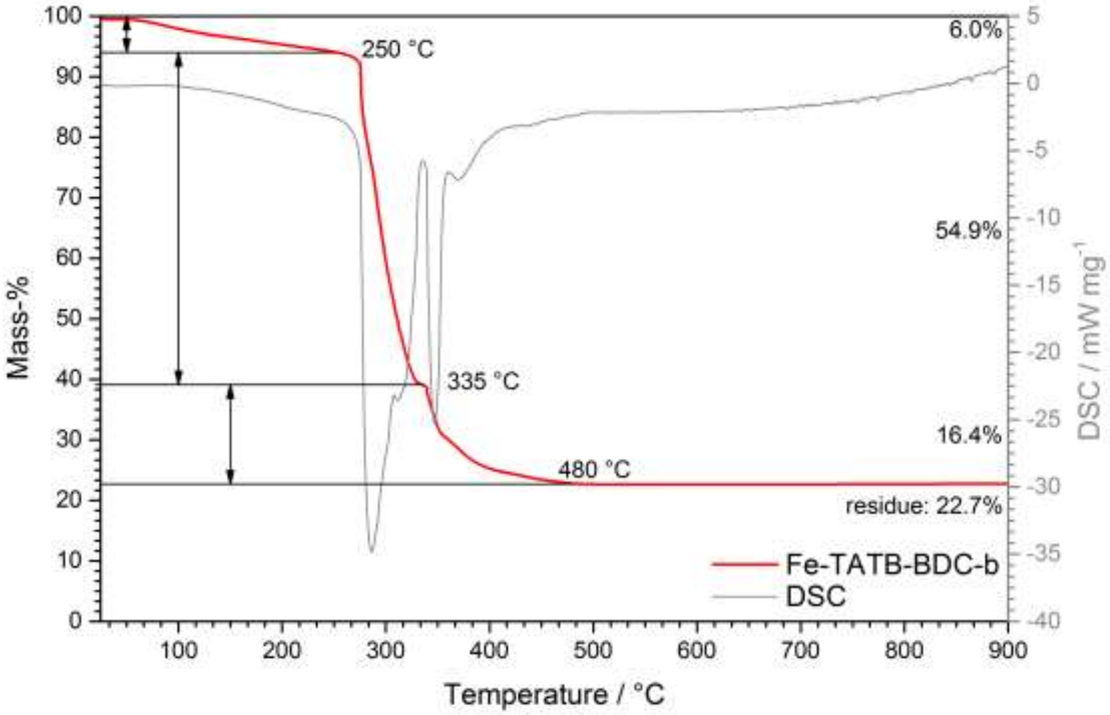

Figure S9: Results of thermogravimetric analysis (red curve) and differential scanning calorimetry (light gray curve) of Fe-TATB-BDC-b in flowing air with a heating rate of 10 ^{o}C min^{-1}. Prior to the TGA/DSC measurement, the material had been used for the nitrogen sorption experiments. The start temperature of the decomposition and the mass loss of individual steps are indicated.

Table S2: Mass-losses of Fe-TATB-BDC-b during thermogravimetric analysis: experimentally determined data (Figure S9), experimentally determined data taking the content of guests into account, and calculated data based on the ideal composition of Fe-TATB-BDC-b [$Fe_3O(Cl)(H_2O)_2(BDC\text{-}NH_2)_{3/2}(TATB)$].

	experimental	guest free	calculated
guest	6.0%		
linker	71.3%	75.8%	75.1%
residue	22.7%	24.2%	24.9%

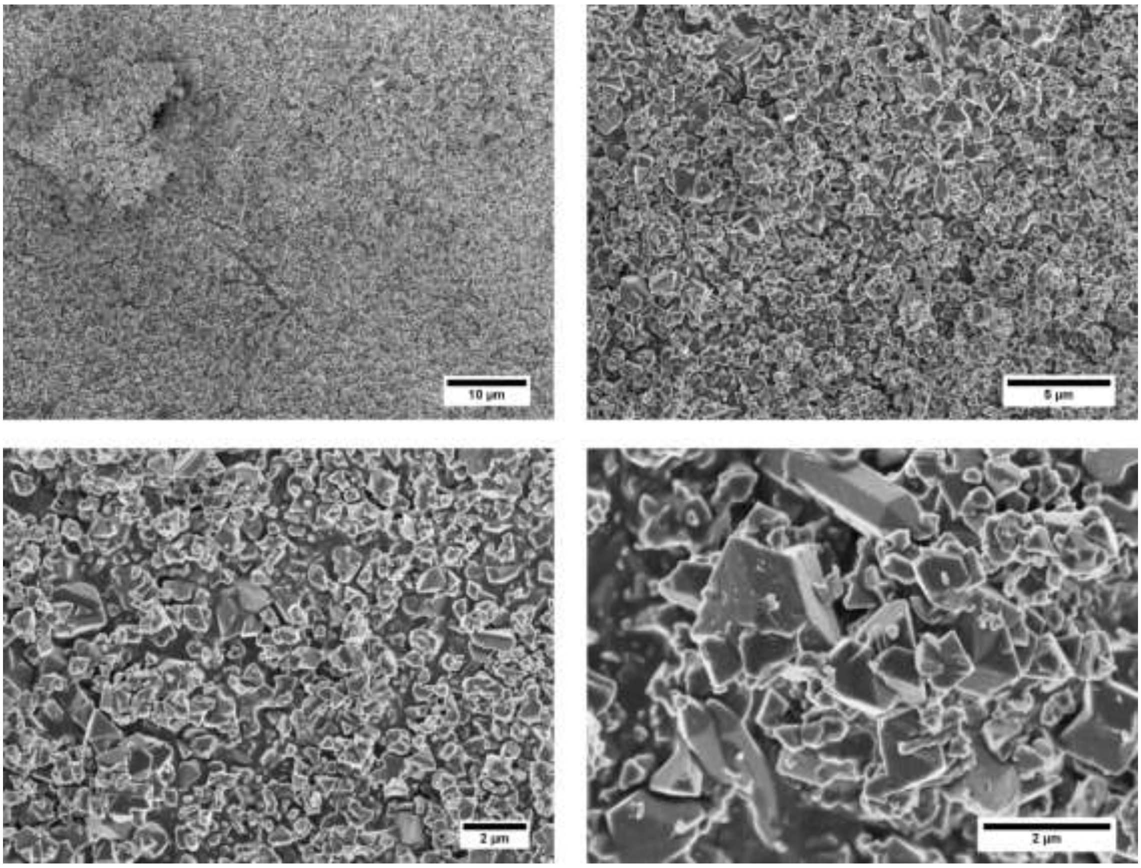

Figure S10: SEM images of the Fe-TATB-BDC-b recorded at different magnifications, showing randomly shaped particles with similar crystallite sizes.

Fe-TATB-BDC-c

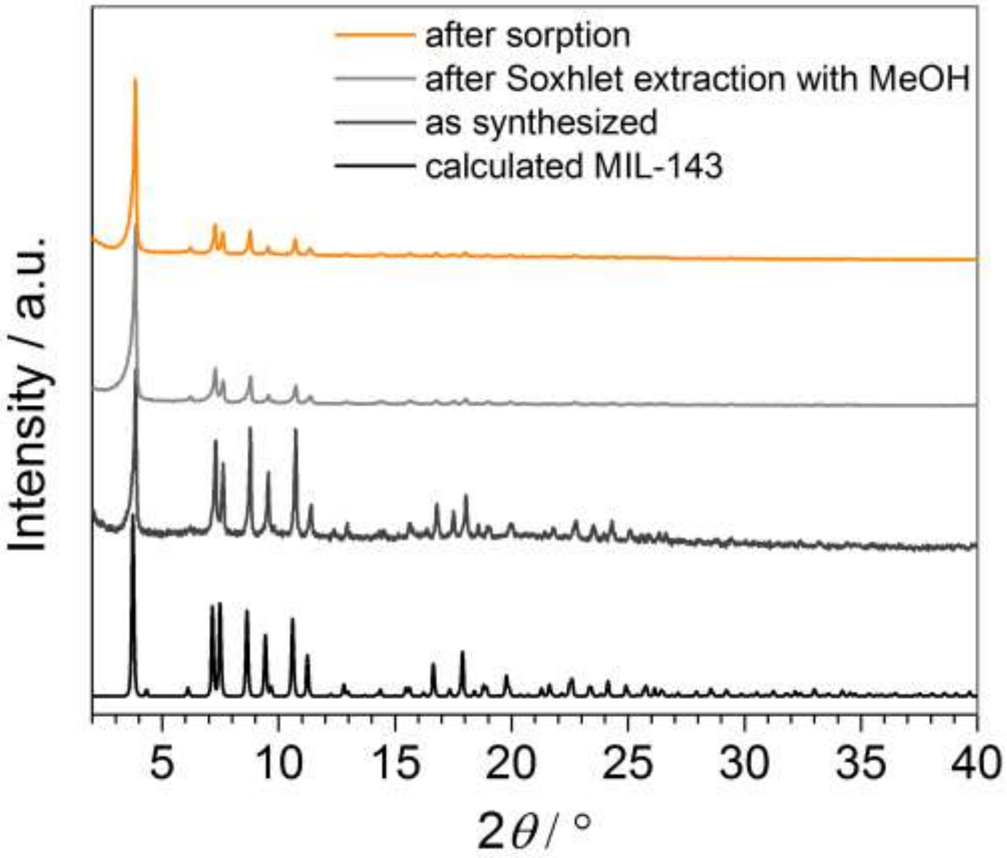

Figure S11: PXRD patterns of Fe-TATB-BDC-c as synthesized (dark gray), after Soxhlet extraction with methanol (light gray), and after sorption isotherm measurement (orange) are compared to the calculated pattern of MIL-143 (black). All data are from the same synthesis batch.

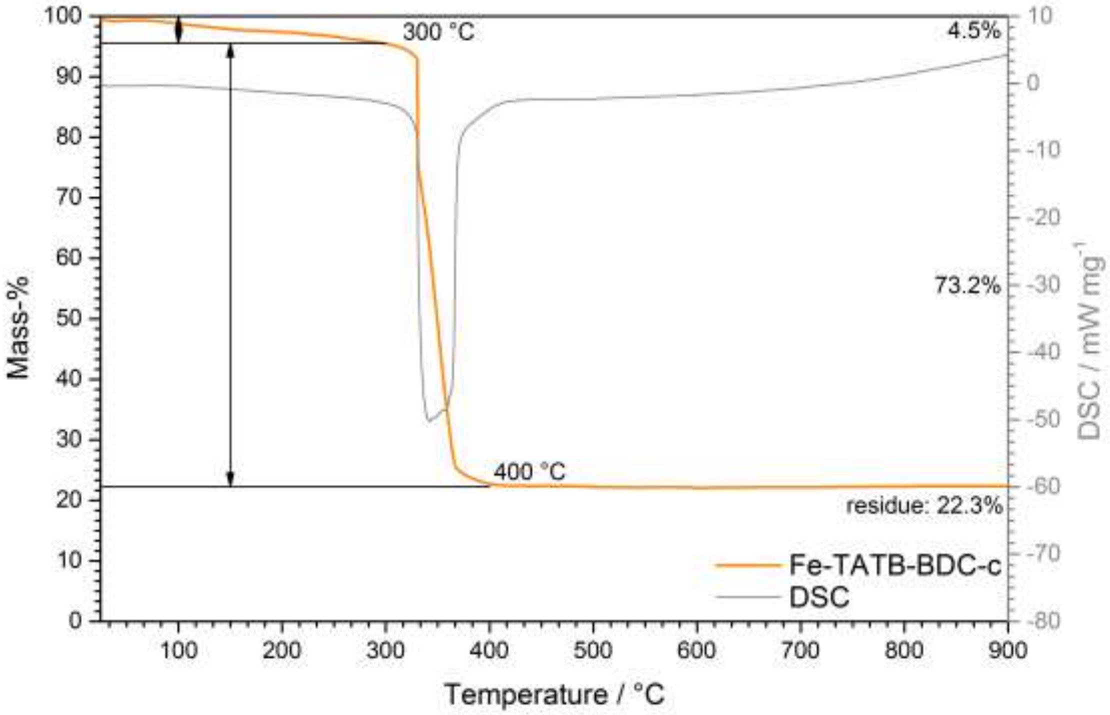

Figure S12: Results of thermogravimetric analysis (orange curve) and differential scanning calorimetry (light gray curve) of Fe-TATB-BDC-c in flowing air with a heating rate of 10 ^{o}C min^{-1}. Prior to the TGA/DSC measurement, the material had been used for the nitrogen sorption experiments. The start temperature of the decomposition and the mass loss of individual steps are indicated.

Table S3: Mass-losses of Fe-TATB-BDC-c during thermogravimetric analysis: experimentally determined data (Figure S12), experimentally determined data taking the content of guests into account, and calculated data based on the ideal composition of Fe-TATB-BDC-c [$Fe_3O(Cl)(H_2O)_2(BDC)_{3/2}(TATB\text{-}NO_2(\textit{meta}))$].

	experimental	**guest free**	**calculated**
guest	4.5%		
linker	73.2%	76.6%	75.7%
residue	22.3%	23.4%	24.3%

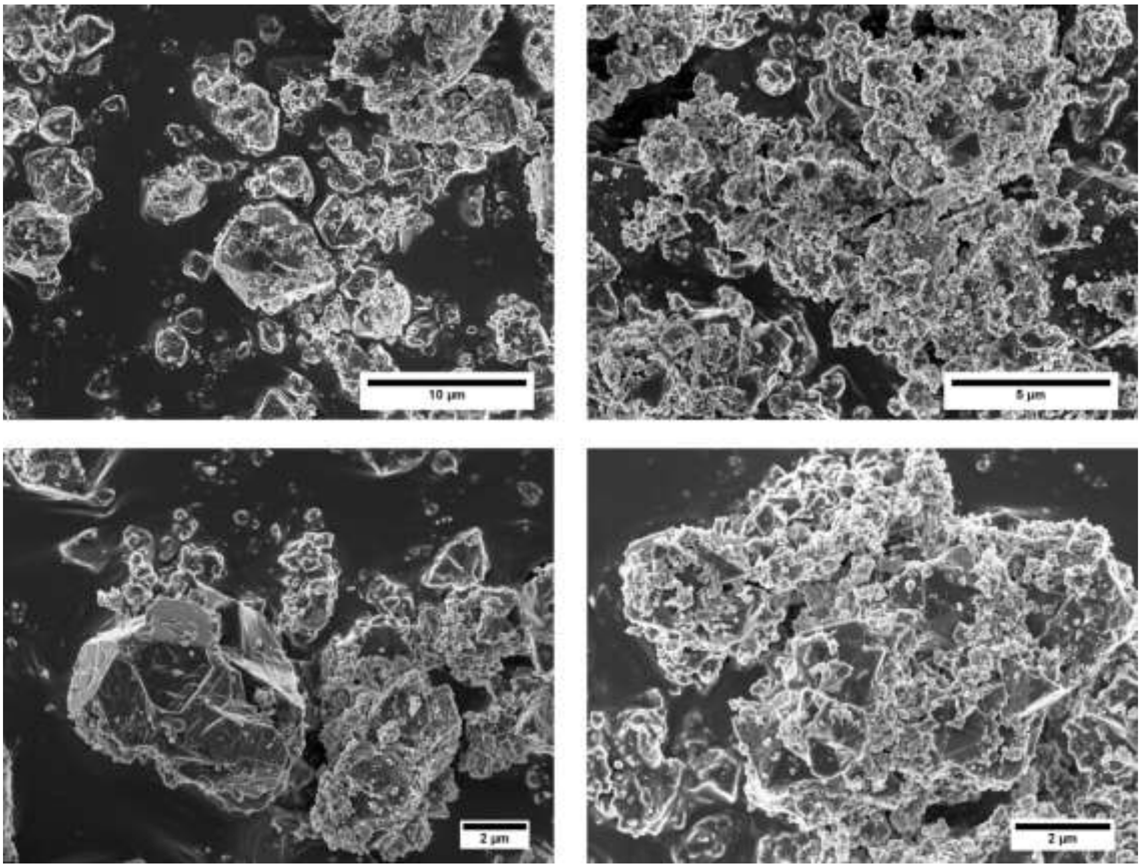

Figure S13: SEM images of the Fe-TATB-BDC-c recorded at different magnifications, showing randomly shaped particles with small and large crystallite sizes.

Fe-TATB-BDC-d

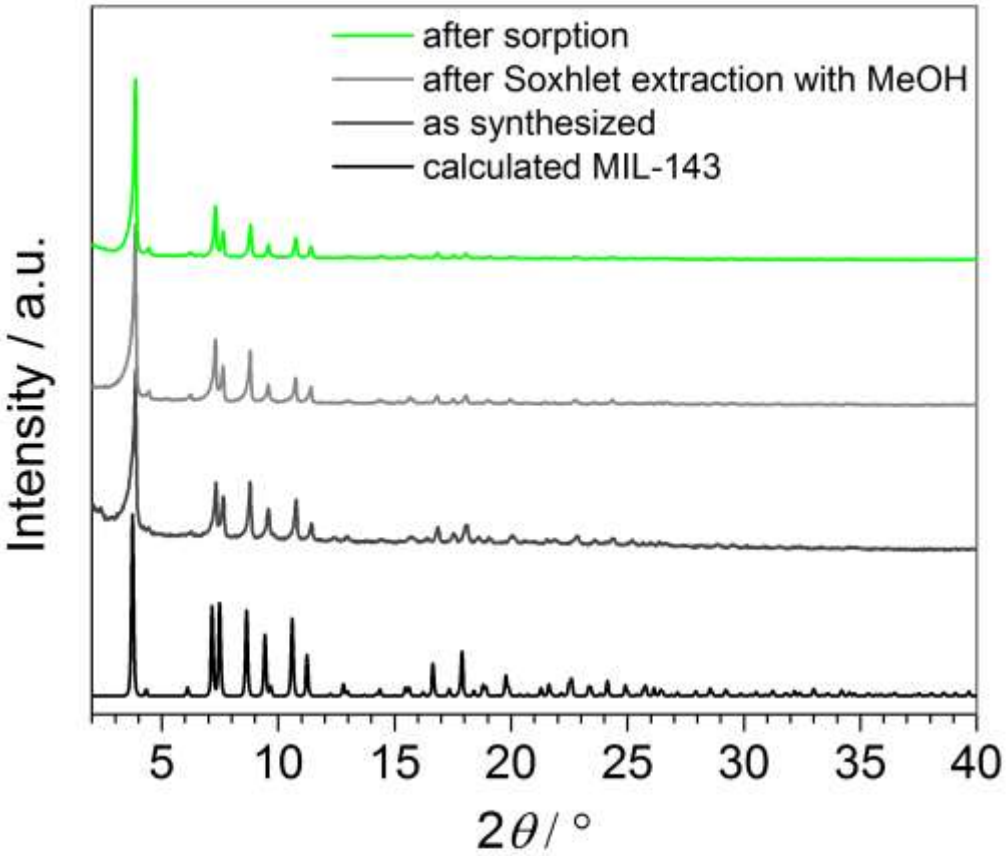

Figure S14: PXRD patterns of Fe-TATB-BDC-d as synthesized (dark gray), after Soxhlet extraction with methanol (light gray), and after sorption isotherm measurement (light green) are compared to the calculated pattern of MIL-143 (black). All data are from the same synthesis batch.

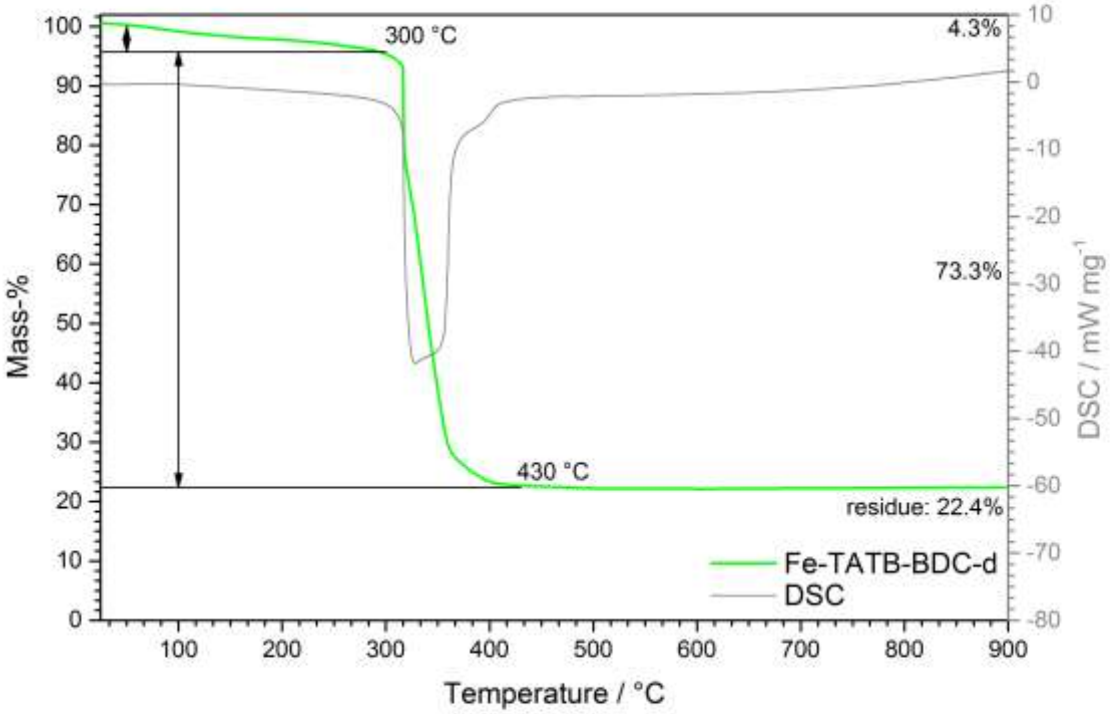

Figure S15: Results of thermogravimetric analysis (light green curve) and differential scanning calorimetry (light gray curve) of Fe-TATB-BDC-d in flowing air with a heating rate of 10 ^{o}C min^{-1}. Prior to the TGA/DSC measurement, the material had been used for the nitrogen sorption experiments. The start temperature of the decomposition and the mass loss of individual steps are indicated.

Table S4: Mass-losses of Fe-TATB-BDC-d during thermogravimetric analysis: experimentally determined data (Figure S15), experimentally determined data taking the content of guests into account, and calculated data based on the ideal composition of Fe-TATB-BDC-d [$Fe_3O(Cl)(H_2O)_2(BDC)_{3/2}$(TATB-$NO_2$(*ortho*))].

	experimental	**guest free**	**calculated**
guest	4.3%		
linker	73.3%	76.6%	75.7%
residue	22.4%	23.4%	24.3%

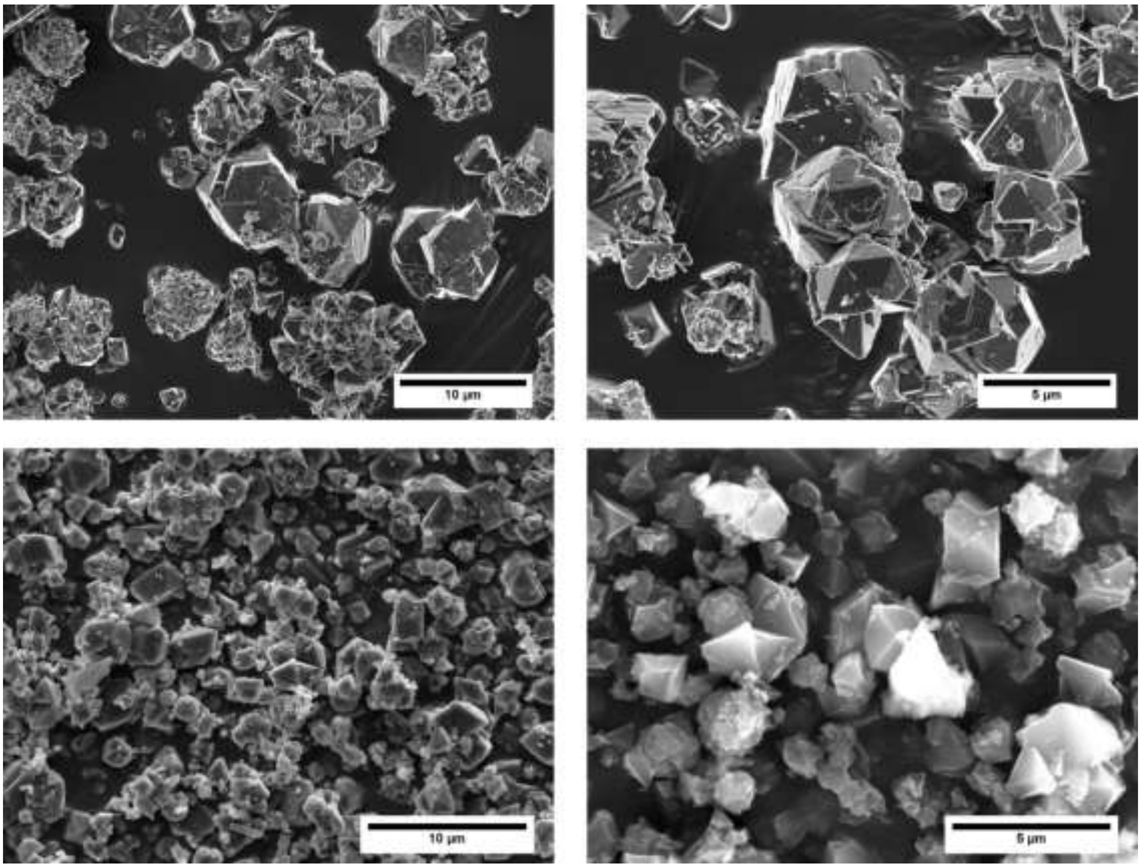

Figure S16: SEM images of the Fe-TATB-BDC-d recorded at different magnifications, showing randomly shaped particles with small and large crystallite sizes.

Fe-TATB-BDC-e

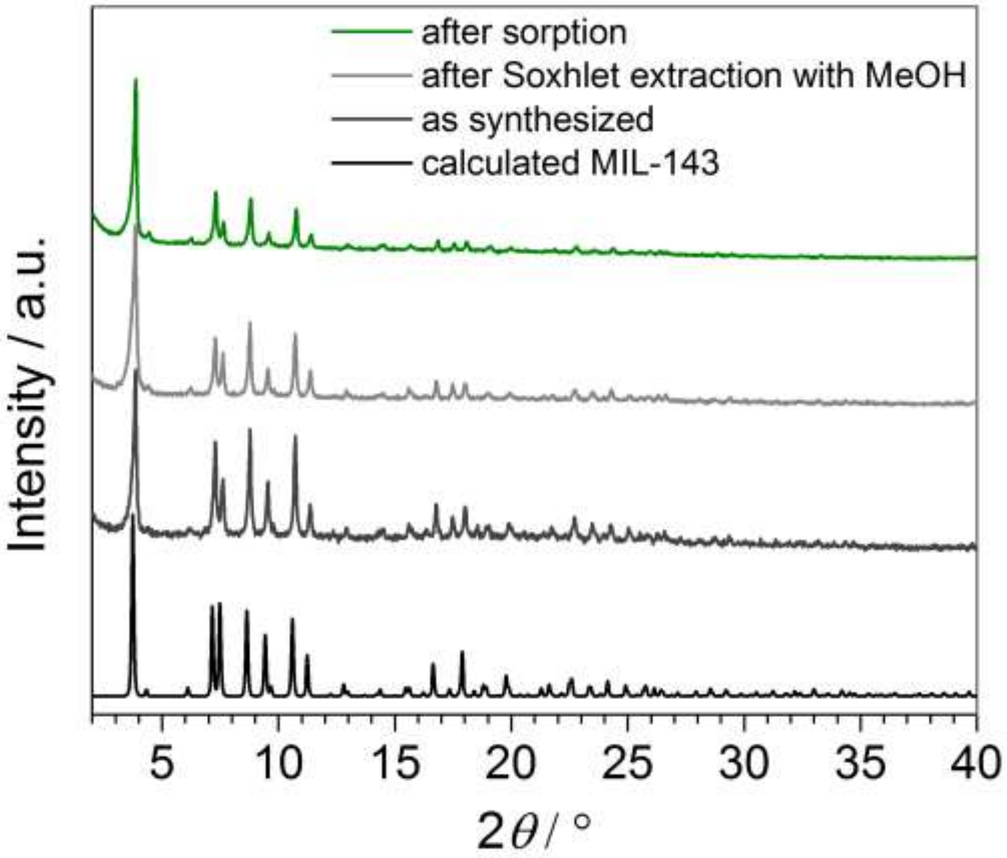

Figure S17: PXRD patterns of Fe-TATB-BDC-e as synthesized (dark gray), after Soxhlet extraction with methanol (light gray), and after sorption isotherm measurement (dark green) are compared to the calculated pattern of MIL-143 (black). All data are from the same synthesis batch.

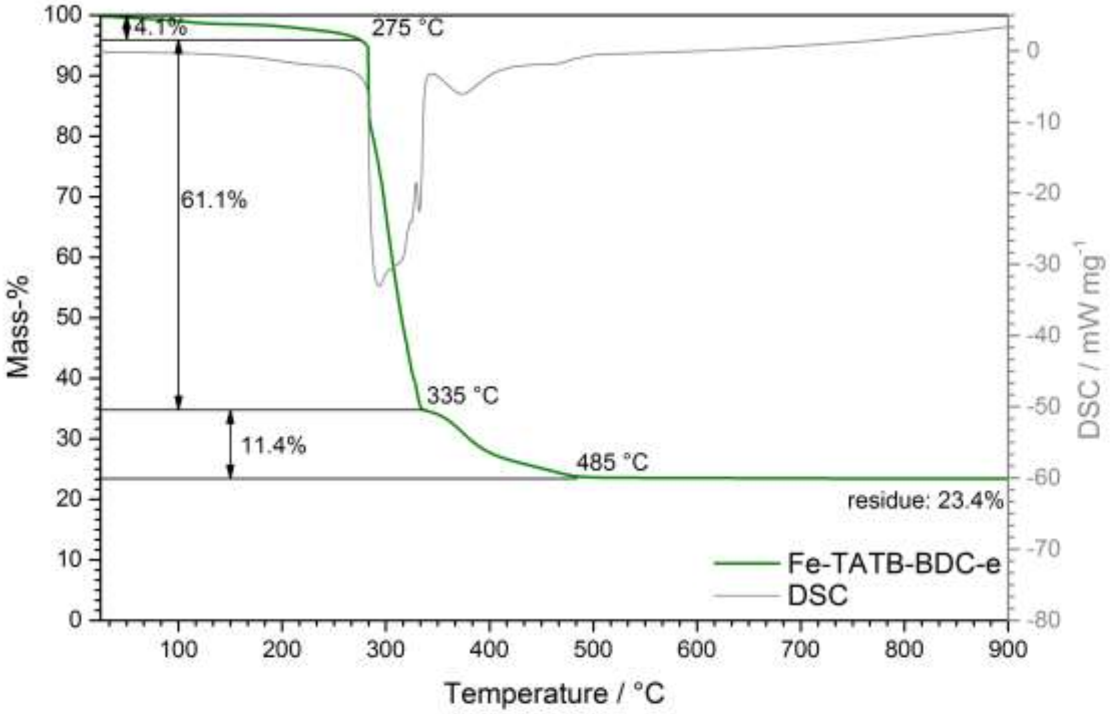

Figure S18: Results of thermogravimetric analysis (dark green curve) and differential scanning calorimetry (light gray curve) of Fe-TATB-BDC-e in flowing air with a heating rate of 10 °C min^{-1}. Prior to the TGA/DSC measurement, the material had been used for the nitrogen sorption experiments. The start temperature of the decomposition and the mass loss of individual steps are indicated.

Table S5: Mass-losses of Fe-TATB-BDC-e during thermogravimetric analysis: experimentally determined data (Figure S18), experimentally determined data taking the content of guests into account, and calculated data based on the ideal composition of Fe-TATB-BDC-e [$Fe_3O(Cl)(H_2O)_2(BDC\text{-}NH_2)_{3/2}(TATB\text{-}NO_2$(*meta*))].

	experimental	**guest free**	**calculated**
guest	4.1%		
linker	72.5%	75.6%	76.2%
residue	23.4%	24.4%	23.8%

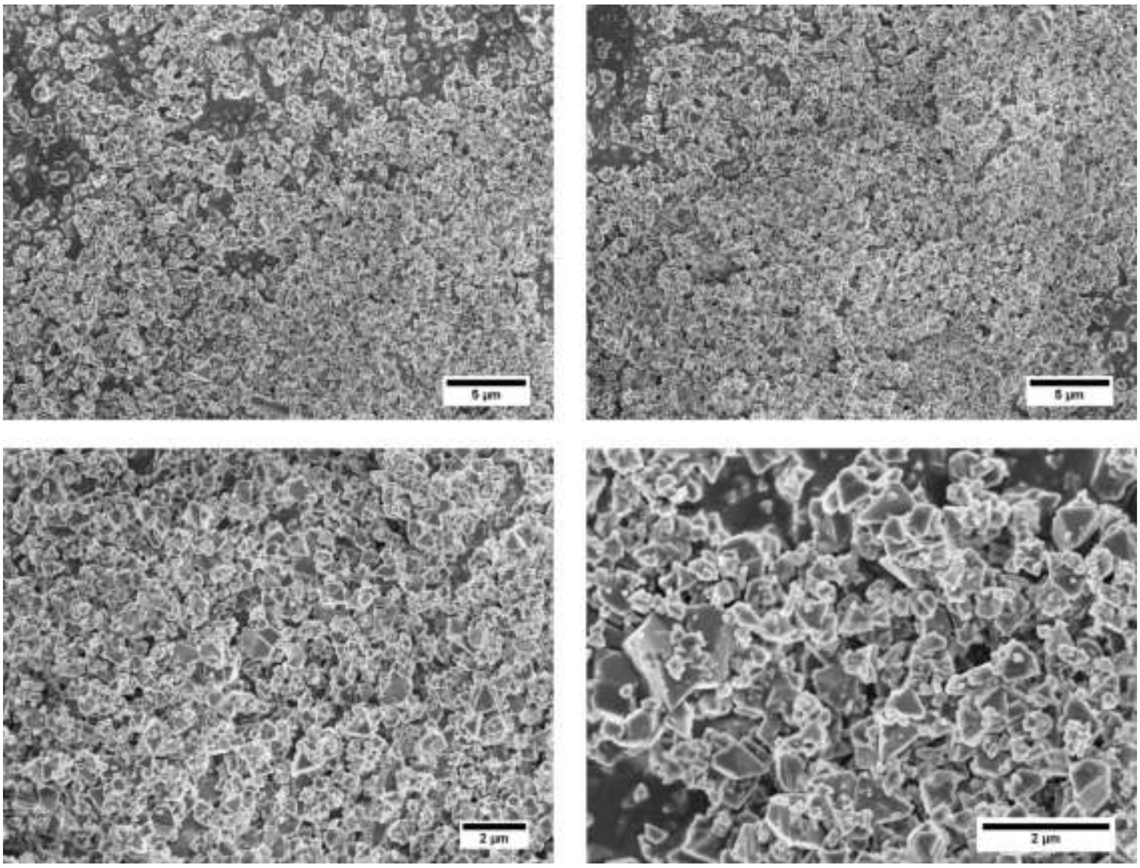

Figure S19: SEM images of the Fe-TATB-BDC-e recorded at different magnifications, showing randomly shaped particles with similar crystallite sizes.

Fe-TATB-BPDC

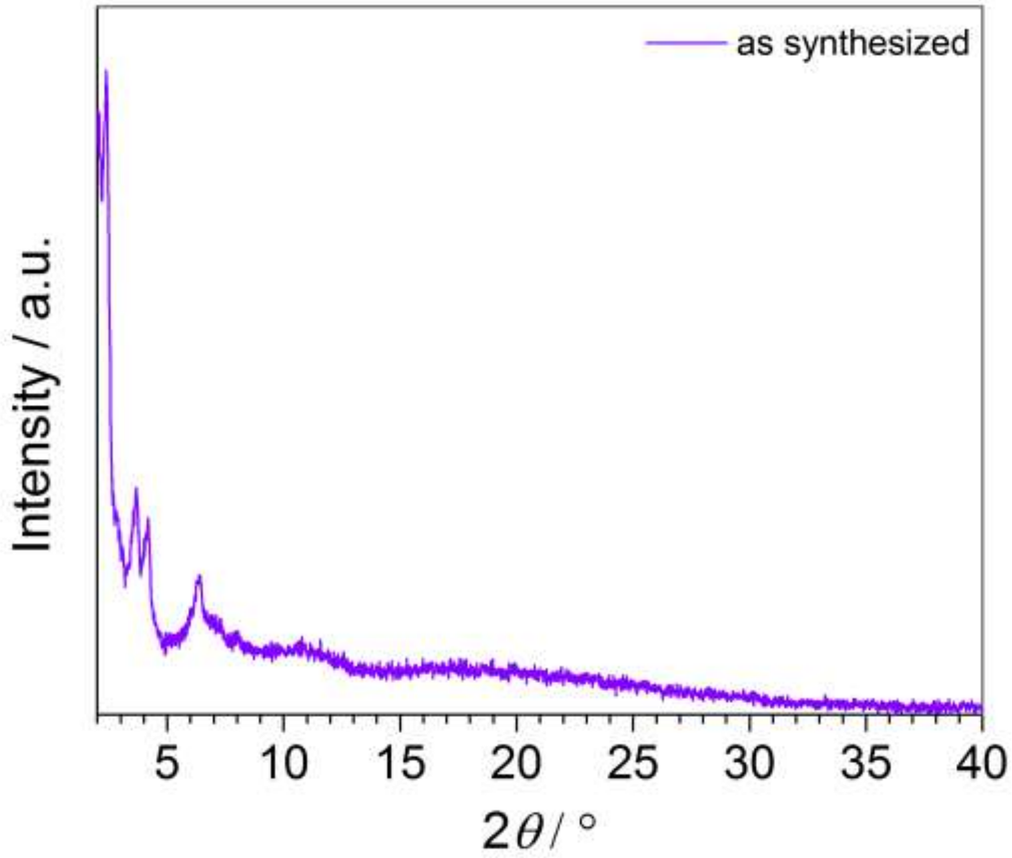

Figure S20: PXRD pattern of Fe-TATB-BPDC as synthesized (purple).

Fe-TAPB-BDC

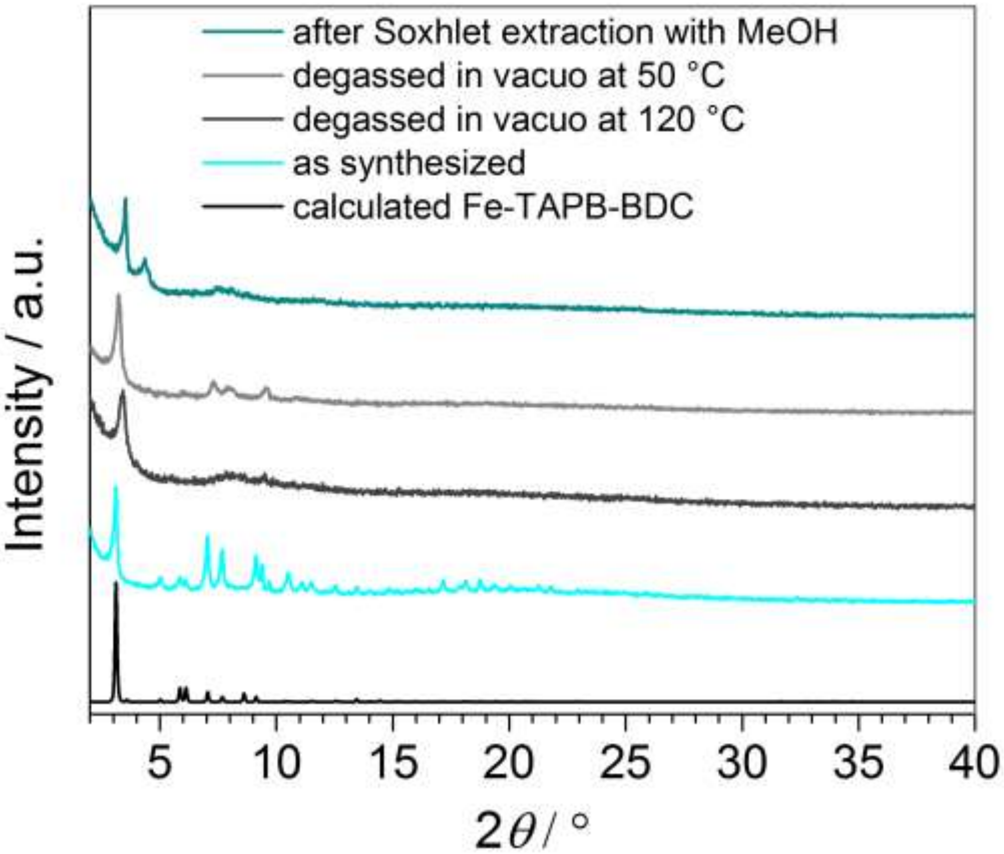

Figure S21: PXRD patterns of Fe-TAPB-BDC as synthesized (cyan), after at 120 °C in vacuo (dark gray), after degassing the sample at only 50 °C in vacuo (light gray) and after Soxhlet extraction with methanol (dark cyan) are compared to a calculated pattern with MIL-143 topology (black; for details see page 4). For testing the different activation conditions only a few mg of the samples were used. And all tested conditions can be referred to the as synthesized sample.

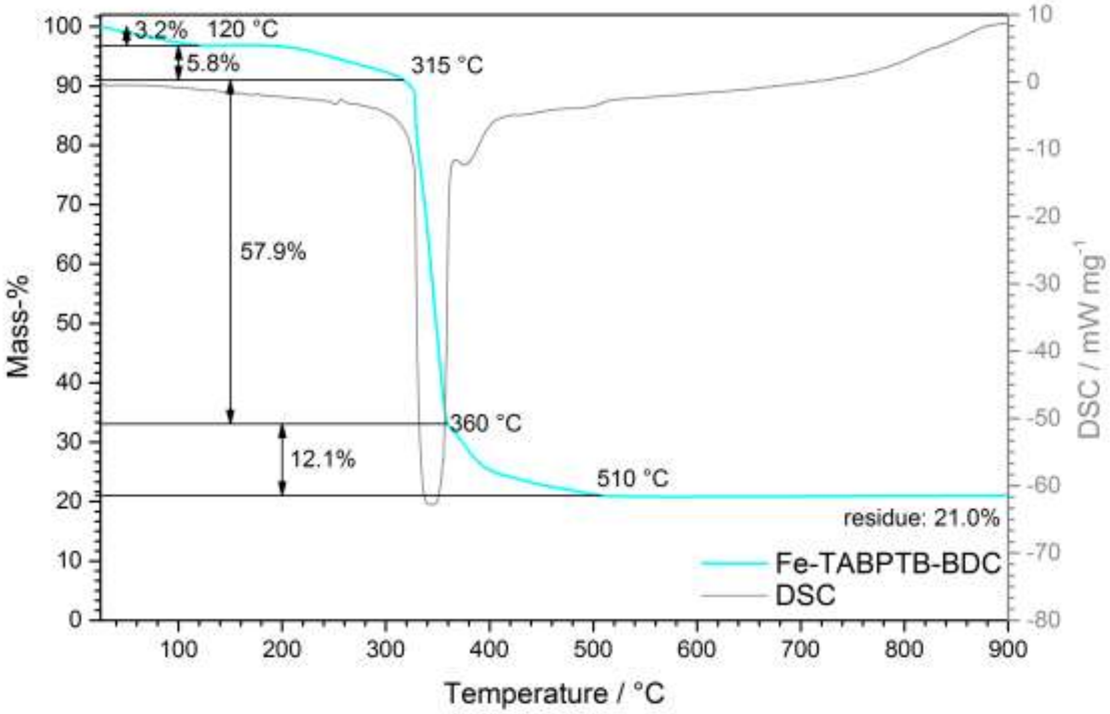

Figure S22: Results of thermogravimetric analysis (cyan curve) and differential scanning calorimetry (light gray curve) of Fe-TAPB-BDC in flowing air with a heating rate of 10 °C min^{-1}. The start temperature of the decomposition and the mass loss of individual steps are indicated.

Table S6: Mass-losses of Fe-TAPB-BDC during thermogravimetric analysis: experimentally determined data (Figure S22), experimentally determined data taking the content of guests into account, and calculated data based on the ideal composition of Fe-TAPB-BDC [$Fe_3O(Cl)(H_2O)_2(BDC)_{3/2}(TAPB)$].

	experimental	guest free	calculated
guest	9.0%		
linker	70.0%	76.9%	80.0%
residue	21.0%	23.1%	20.0%

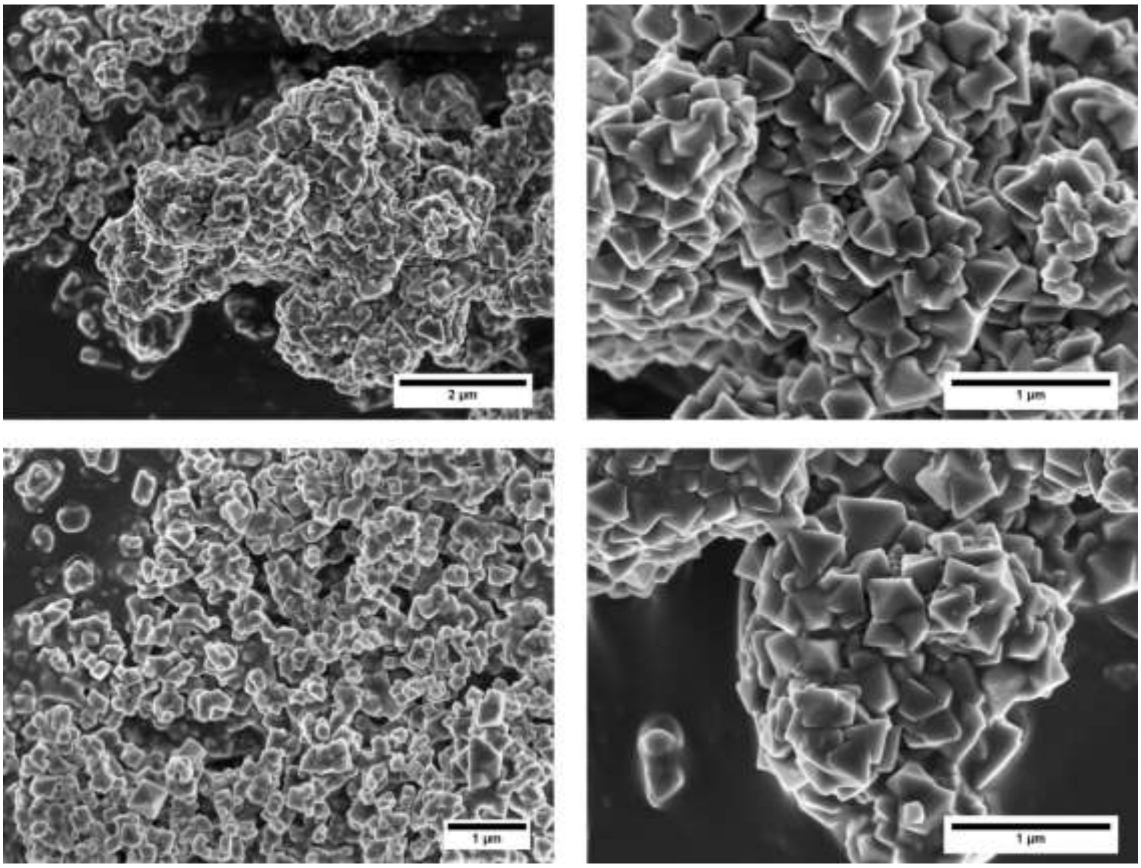

Figure S23: SEM images of the Fe-TAPB-BDC recorded at different magnifications, showing randomly shaped particles with similar crystallite sizes.

Fe-TAPB-BPDC

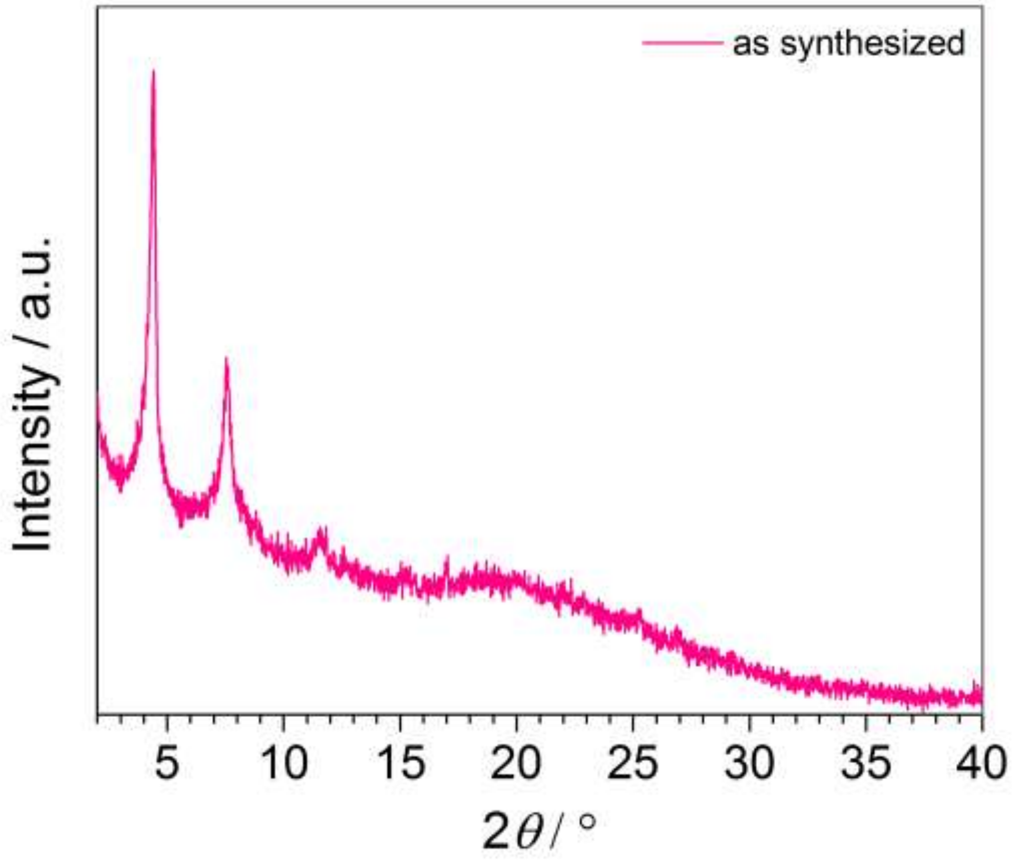

Figure S24: PXRD patterns of Fe-TAPB-BPDC as synthesized (pink).

Fe-BTB-BDC

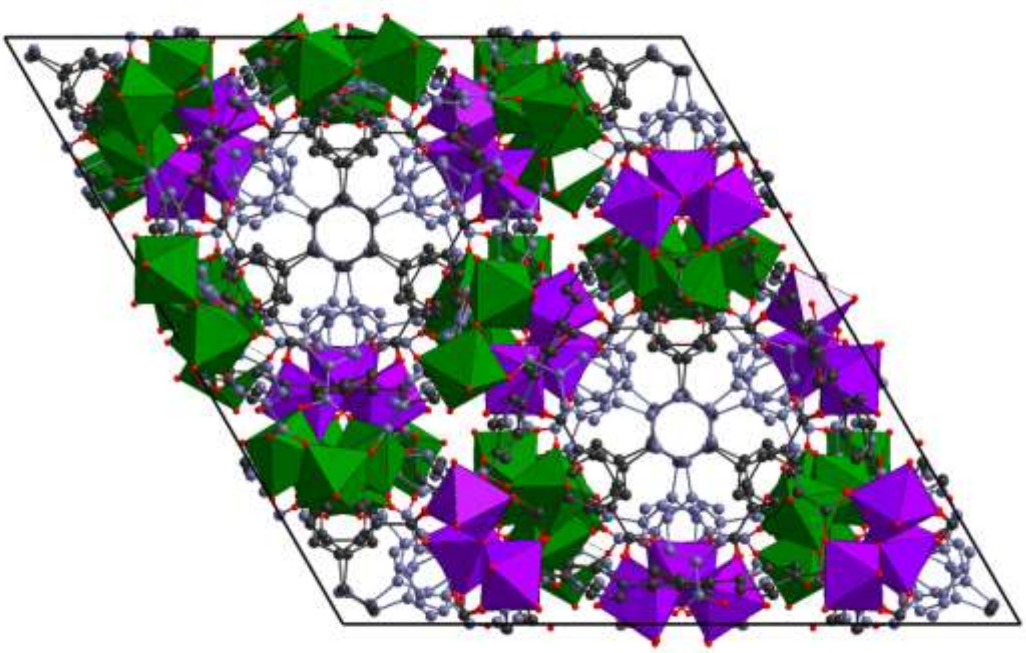

Figure S25: View of the MIL-142 framework along [001]. The interpenetration in MIL-142 by two individual networks is represented by the two different colours of the FeO_6 octahedra (purple and green) and carbon atoms (grey and grey blue); carbon (grey and blue grey spheres), oxygen (red spheres), hydrogen atoms have been omitted for clarity.

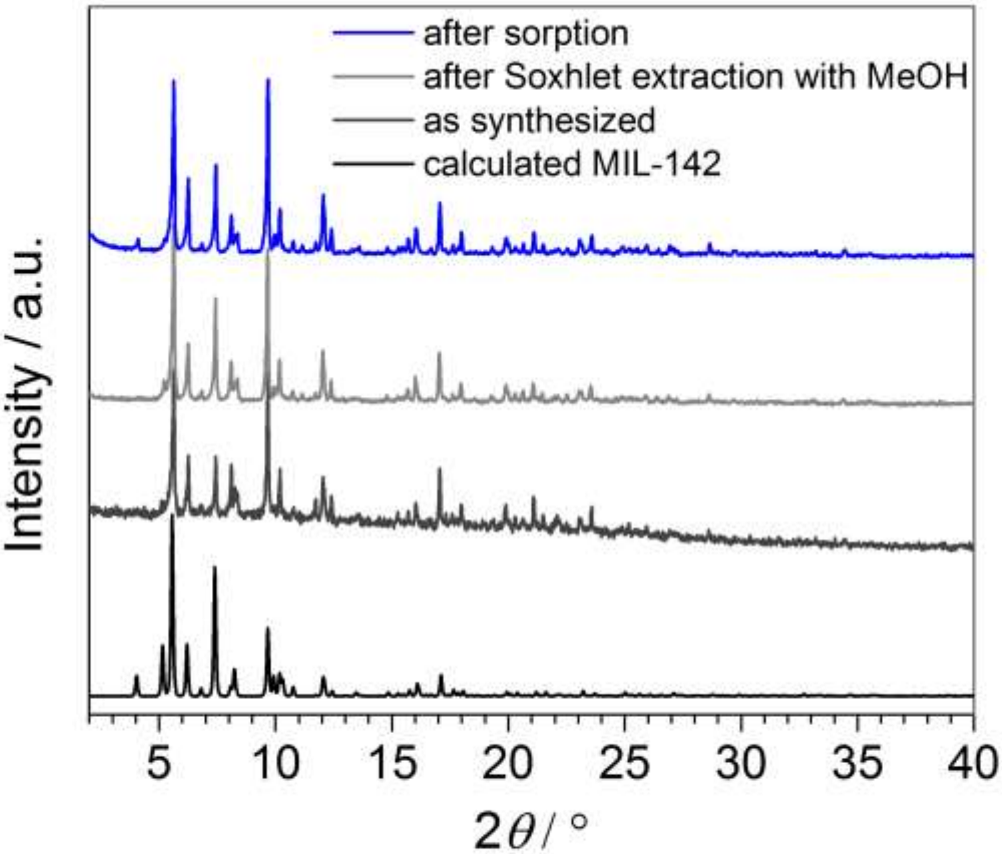

Figure S26: PXRD patterns of Fe-BTB-BDC as synthesized (dark gray), after Soxhlet extraction with methanol (light gray), and after sorption isotherm measurement (blue) are compared to the calculated pattern of MIL-142 (black). All data are from the same synthesis batch.

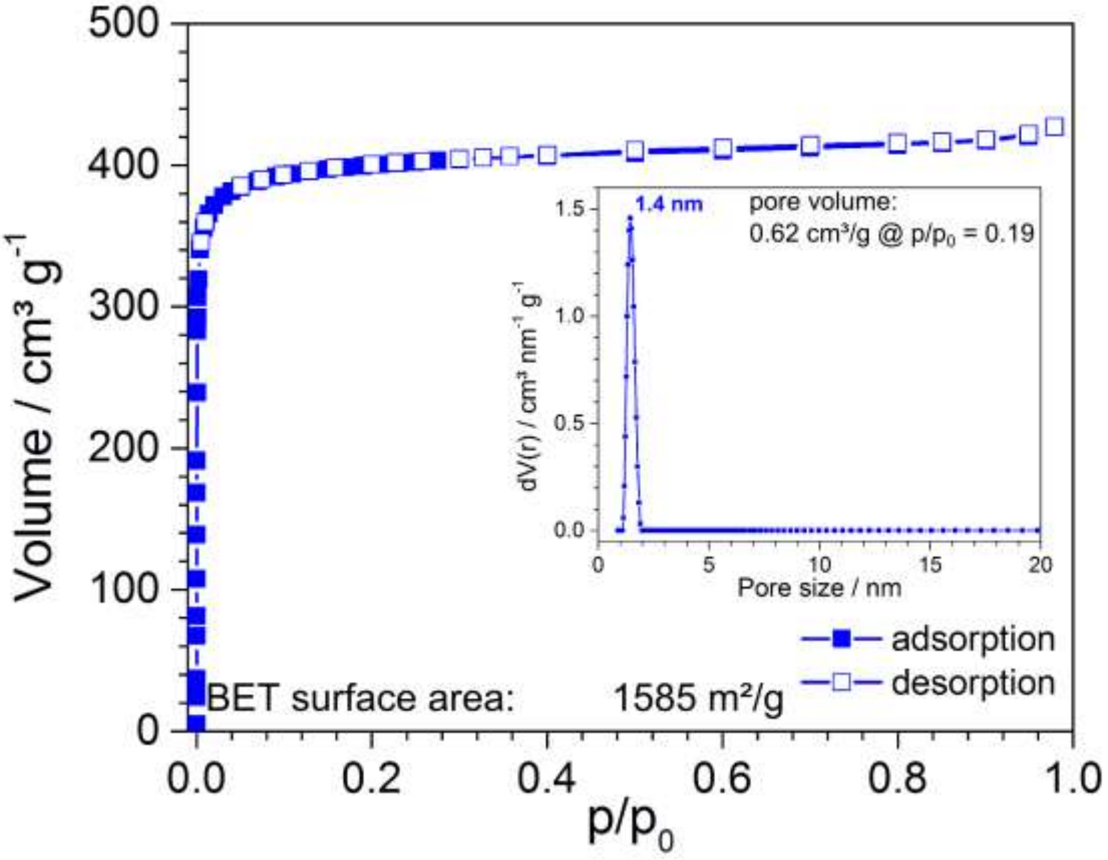

Figure S27: N_2 sorption isotherm of Fe-BTB-BDC at 77 K with the adsorption denoted by filled symbols and desorption by empty symbols. The insert shows the pore size distribution and was calculated with the QSDFT model using cylindrical and sphere pores at the adsorption branch. Also the BET surface area as well as the pore volume are reported.

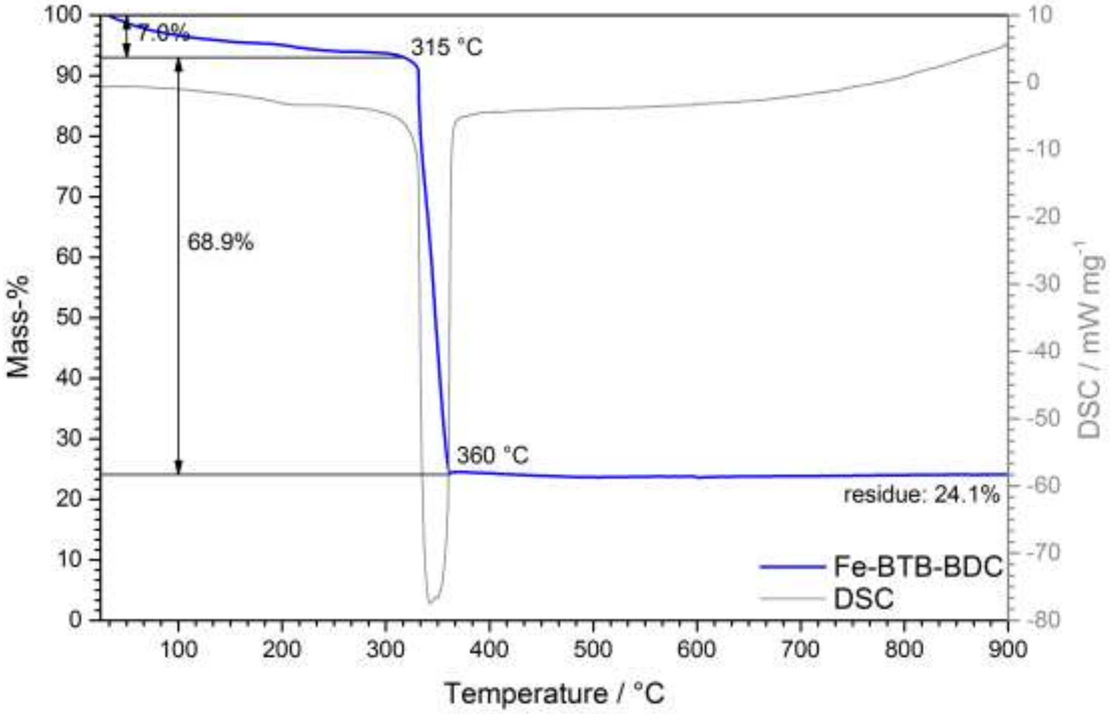

Figure S28: Results of thermogravimetric analysis (blue curve) and differential scanning calorimetry (light gray curve) of Fe-BTB-BDC in flowing air with a heating rate of 10 °C min^{-1}. Prior to the TGA/DSC measurement, the material had been used for the nitrogen sorption experiments. The start temperature of the decomposition and the mass loss of individual steps are indicated.

Table S7: Mass-losses of Fe-BTB-BDC during thermogravimetric analysis: experimentally determined data (Figure S28), experimentally determined data taking the content of guests into account, and calculated data based on the ideal composition of Fe-BTB-BDC [$Fe_3O(Cl)(H_2O)_2(BDC)(BTB)_{4/3}$].

	experimental	**guest free**	**calculated**
guest	7.0%		
linker	68.9%	74.1%	75.8%
residue	24.1%	25.9%	24.2%

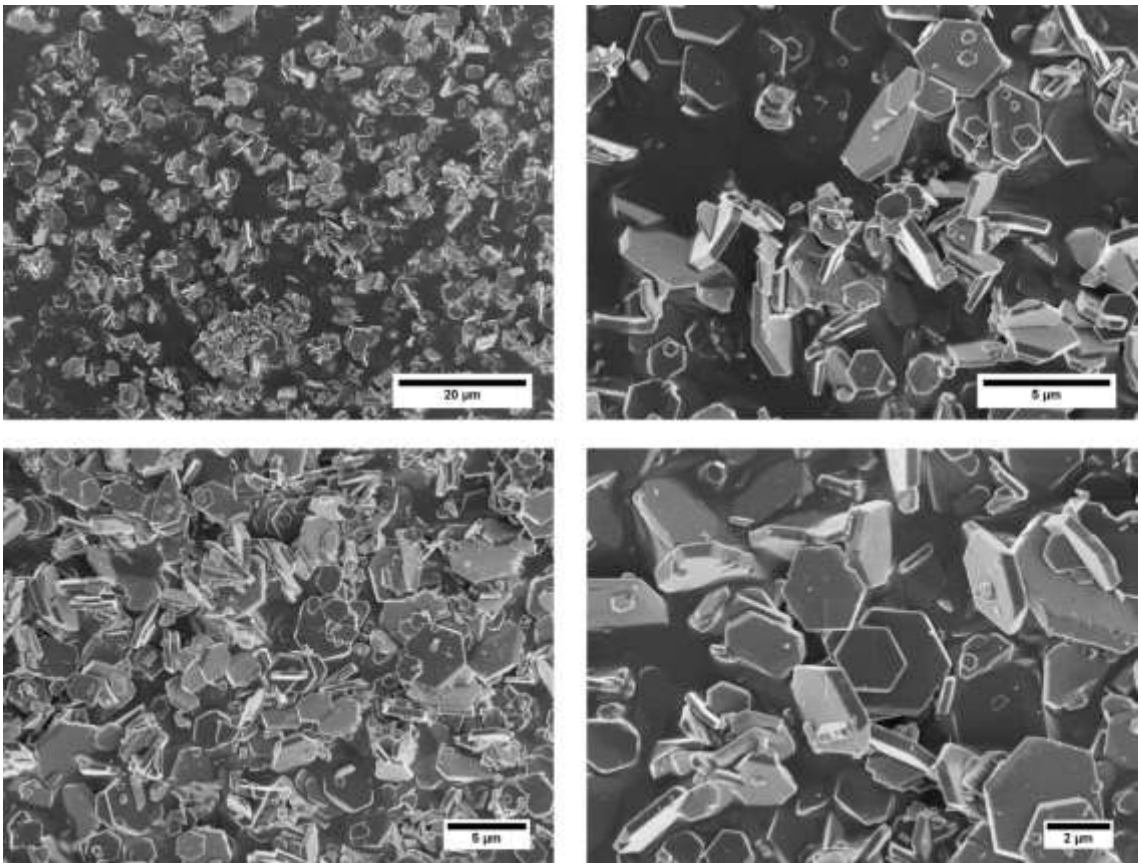

Figure S29: SEM images of the Fe-BTB-BDC recorded at different magnifications, showing hexagonal shaped plate-like-particles with different crystallite sizes.

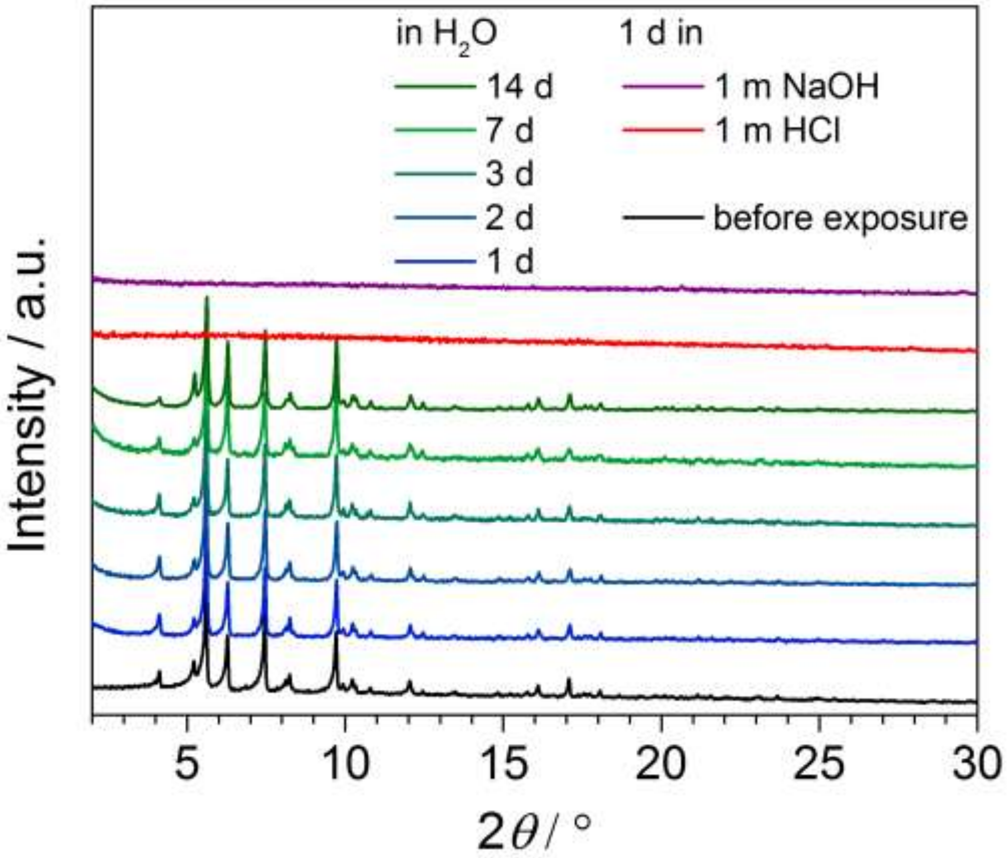

Figure S30: PXRD measurement of Fe-BTB-BDC before exposure (black curve) is compared to the PXRD plots after the exposure to Millipore water with different times of exposure (1 d, 2d, 3 d, 7d, 14 d; blue and green curve, respectively). Also the exposure to a 1 M hydrochloric acid (red curve) and to a 1 M sodium hydroxide (purple curve) solution for 1 d are presented here. The framework is stable up to 7 d in water, while the framework decomposes under acidic and basic conditions.

Table S8: Summary of *Le Bail* fits of PXRD data.

	Instrument	**MIL-142 (*R*3*c*, no. 161)**	**MIL-143 (*F*23, no. 196)**
Fe-TATB-BDC-a	Stoe data (RT)	Minor amounts	a = 40.623(3) Å V = 67039(14) Å^3
	ESRF data (RT, 3 scans)	Minor amounts	a = 40.254(8) Å V = 65230(40) Å^3
	ESRF data (100 K, 5 scans)	Minor amounts	a = 40.308(8) Å V = 65490(40) Å^3
Fe-TATB-BDC-b	Stoe data (RT)	None	a = 40.606(2) Å V = 66955(12) Å^3
	ESRF data (RT, 7 scans)	None	a = 40.332(4) Å V = 65610(20) Å^3
Fe-TATB-BDC-c	Stoe data (RT)	None	a = 40.770(2) Å V = 67768(8) Å^3
Fe-TATB-BDC-d	Stoe data (RT)	None	a = 40.649(2) Å V = 67165(8) Å^3
	ESRF data (RT, 4 scans)	None	a = 40.369(10) Å V = 65790(50) Å^3
Fe-TATB-BDC-e	Stoe data (RT)	Minor amounts	a = 40.603(3) Å V = 66936(15) Å^3
	ESRF data (RT, 1 scan)	Minor amounts	a = 40.392(6) Å V = 65900(30) Å^3
	ESRF data (100 K, 5 scans)	Minor amounts	a = 40.388(9) Å V = 65880(40) Å^3
Fe-BTB-BDC	Stoe data (RT)	a = 28.801(1) Å c = 96.040(6) Å V = 68993(7) Å^3	None

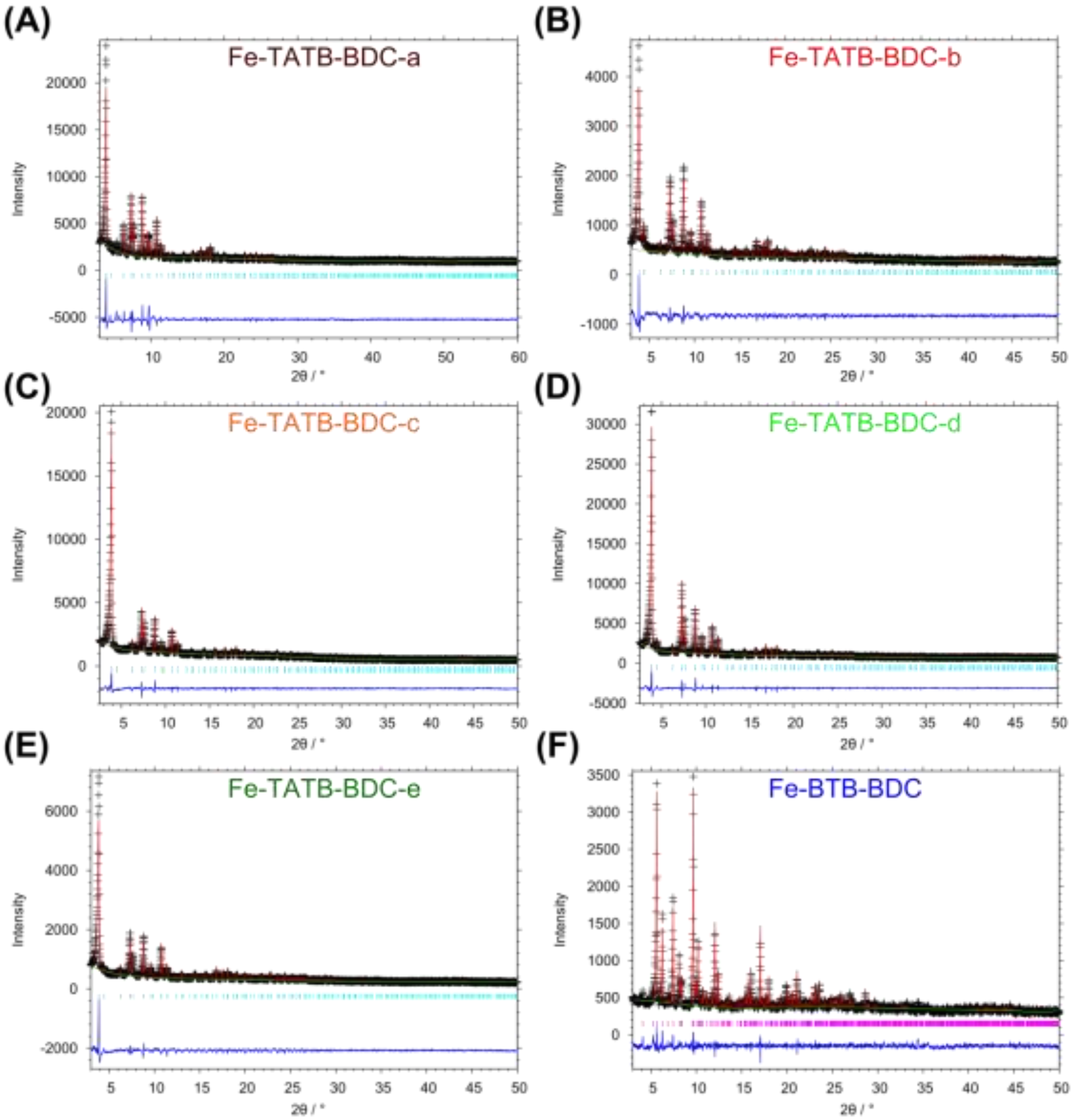

Figure S31: Plots of *Le Bail* fits of PXRD data recorded with a Stoe Stadi P diffractometer (RT, CuKα_1 radiation, flat sample). a) Fe-TATB-BDC-a, b) Fe-TATB-BDC-b, c) Fe-TATB-BDC-c, d) Fe-TATB-BDC-d, e) Fe-TATB-BDC-e and f) Fe-BTB-BDC.

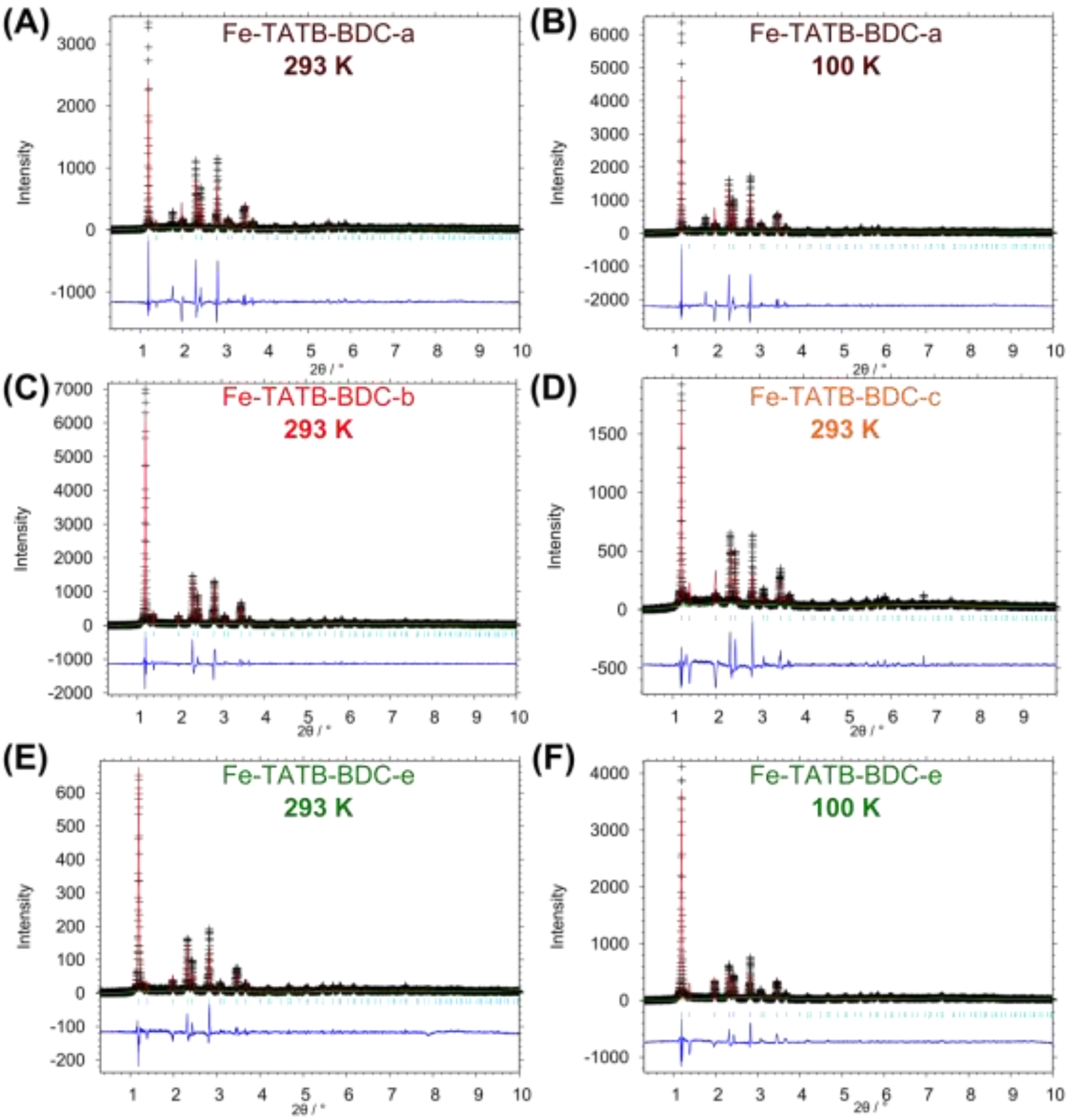

Figure S32: Plots of *Le Bail* fits of synchrotron PXRD data recorded at beamline SNBL BM01b / ESRF (λ = 0.504477 Å, capillary with ∅ = 1.0 mm), either at 298 K or 100 K. a) Fe-TATB-BDC-a at 298 K, b) Fe-TATB-BDC-a at 100 K, c) Fe-TATB-BDC-b at 298 K, d) Fe-TATB-BDC-c at 298 K, e) Fe-TATB-BDC-e at 298 K and f) Fe-TATB-BDC-e at 100 K.

4. References

[1] W. van Beek, O. V. Safonova, G. Wiker, H. Emerich, *Phase Transitions* **2011**, *84*, 726-732.

[2] H. Chevreau, T. Devic, F. Salles, G. Maurin, N. Stock, C. Serre, *Angew. Chem. Int. Ed.* **2013**, *52*, 5056-5060.

[3] A. C. Larson, R. B. Von Dreele, *Los Alamos Laboratory, Rep. No. LA-UR* **1987**, *86*, 748.

[4] P.-E. Werner, L. Eriksson, M. Westdahl, *J. Appl. Crystallogr.* **1985**, *18*, 367-370.

[5] D. Klank, *Partikelwelt* **2003**, *2*, 6-7.

[6] K. S. Walton, R. Q. Snurr, *J. Am. Chem. Soc.* **2007**, *129*, 8552-8556.

[7] A. Klinkebiel, O. Beyer, B. Malawko, U. Lüning, *Beilstein J. Org. Chem.* **2016**, *12*, 2267-2273.